Artificial Boundary Conditions for the Numerical Simulation of Unsteady Electromagnetic Waves

S. V. Tsynkov [1]

Department of Mathematics and Center for Research in Scientific Computation (CRSC), North Carolina State University, Box 8205, Raleigh, NC 27695, USA.

Abstract

A central characteristic feature of an important class of hyperbolic PDEs in odd-dimension spaces is *the presence of lacunae*, i.e., sharp aft fronts of the waves, in their solutions. This feature, which is often associated with the Huygens' principle, is employed to construct accurate non-local artificial boundary conditions (ABCs) for the Maxwell equations. The setup includes the propagation of electromagnetic waves from moving sources over unbounded domains. For the purpose of obtaining a finite numerical approximation the domain is truncated, and the ABCs guarantee that the outer boundary be completely transparent for all the outgoing waves. The lacunae-based approach has earlier been used for the scalar wave equation, as well as for acoustics. In the current paper, *we emphasize the key distinctions between those previously studied models and the Maxwell equations of electrodynamics, as they manifest themselves in the context of lacunae-based integration.* The extent of temporal nonlocality of the proposed ABCs is fixed and limited, and this is not a result of any approximation, it is rather an immediate implication of the existence of lacunae. The ABCs can be applied to any numerical scheme that is used to integrate the Maxwell equations. They do not require any geometric adaptation, and they guarantee that the accuracy of the boundary treatment will not deteriorate even on long time intervals. The paper presents a number of numerical demonstrations that corroborate the theoretical design features of the boundary conditions.

Key words: Electromagnetic waves, Maxwell's equations, unsteady propagation, unbounded domains, truncation, finite computational domain, lacunae, non-deteriorating method, long-term numerical integration.

1 Introduction

Sharp aft fronts of the waves, or lacunae, is a unique feature of certain hyperbolic solutions in odd-dimension spaces. The corresponding class of PDEs includes the Maxwell equations of electrodynamics studied in the current paper, along with the acoustics system (linearized Euler equations) and the scalar wave equation, that have been analyzed previously, see [1–3]. The key idea of using lacunae for computations is very simple. If the sources of waves are compactly supported in space and time, and if the domain of interest has finite size, then it will completely fall inside the lacuna once a certain time interval has elapsed since the inception of the sources. This interval can be easily evaluated ahead of time, and for all subsequent moments of time the solution on the domain of interest will be zero, as this domain will already be behind the aft front of the waves. Therefore, no computation will need to be run any further, which puts a cap on the long-term error build-up. Moreover, during this predetermined finite interval no wave can travel more than a certain distance away in space from the domain of interest. Consequently, a finite auxiliary computational domain can be set up, which facilitates construction of artificial boundary conditions (ABCs). In general, the term "ABCs" is associated with a fairly large group of methods employed for solving infinite-domain problems on the computer. For the purpose of obtaining a finite numerical approximation the original domain is truncated, and the ABCs provide a required closure for the resulting truncated formulation. The literature on the subject of ABCs is broad, and we refer the reader to the review papers [4–6].

It is generally known that highly accurate ABCs are nonlocal. In particular, exact ABCs are always nonlocal in multidimensional settings. For unsteady problems, this also implies nonlocality in time. Nonlocal ABCs may incur high computational costs and require elaborate implementation strategies. As such, local alternatives obtained either independently or as an approximation of nonlocal ABCs conditions, becomes viable. These ABCs are usually inexpensive and easy to implement, but may often lack computational accuracy.

The ABCs for the Maxwell equations that we propose hereafter are nonlocal, and their accuracy can always match that of the interior discretization. However, the extent of their temporal nonlocality is limited, and does not increase as the time elapses. The bound on temporal nonlocality comes as a consequence of the presence of lacunae, i.e., sharp aft fronts of the waves, in the corresponding solutions. In the literature, existence of the lacunae is often referred to in connection with the Huygens' principle.

The lacunae-based ABCs are not limited to the aforementioned case of the compactly supported sources of waves. The case of continuously operating sources, or in general, that of a certain process/phenomenon confined to a

2

bounded region that manifests itself by radiation of electromagnetic waves in the far field, is treated by employing special partitions along the time axis.

Several other nonlocal ABCs' methodologies for unsteady waves have recently been put forward, most notably [7–14]; see also the survey [15]. In comparison, our approach has a number of distinctive characteristics, besides the restricted temporal nonlocality that does not come at a cost of accuracy. The lacunae-based ABCs are obtained directly for the discretization, and can supplement any consistent and stable scheme. In other words, they bypass the common stage of deriving the continuous ABCs and subsequently approximating them, see [5]. The lacunae-based ABCs withstand long-term numerical integration with no deterioration of accuracy and are not restricted geometrically to any particular shape of the external artificial boundary. They also allow one to analyze a variety of cases, including the one of moving sources of waves.

Even though the current ABCs for electromagnetics are related to those developed previously for the scalar wave equation [1, 2] and for acoustics [3], *there are not only similarities but also very important differences between the respective models.* Foremost, the source terms that drive the Maxwell equations are not independent, they are related via the continuity equation. The latter must be enforced on all stages of building the lacunae-based algorithm. In general, the current ABCs' approach fits into the universal framework of [16].

The scope of numerical demonstrations that we present is limited to the transverse magnetic (TM) mode with cylindrical symmetry. This allows us to take advantage of the three-dimensional effects in a two-dimensional setting.

2 Lacunae of the Wave Equation

Consider a three-dimensional wave equation, $\boldsymbol{x} = (x_1, x_2, x_3)$:

$$\frac{1}{c^2}\frac{\partial^2 \varphi}{\partial t^2} - \left(\frac{\partial^2 \varphi}{\partial x_1^2} + \frac{\partial^2 \varphi}{\partial x_2^2} + \frac{\partial^2 \varphi}{\partial x_3^2}\right) = f(\boldsymbol{x}, t), \quad t \geq 0 \tag{1a}$$

$$\left.\varphi\right|_{t=0} = \left.\frac{\partial \varphi}{\partial t}\right|_{t=0} = 0 \tag{1b}$$

with homogeneous initial conditions. For every $(\boldsymbol{x}, t)$, the solution $\varphi = \varphi(\boldsymbol{x}, t)$ of problem (1a), (1b) is given by the Kirchhoff integral (see, e.g., [17]):

$$\varphi(\boldsymbol{x}, t) = \frac{1}{4\pi}\iiint\limits_{\varrho \leq ct} \frac{f\left(\boldsymbol{\xi}, t - \varrho/c\right)}{\varrho}d\boldsymbol{\xi} \tag{2}$$

3

where $\boldsymbol{\xi} = (\xi_1, \xi_2, \xi_3)$, $\varrho = |\boldsymbol{x} - \boldsymbol{\xi}| = \sqrt{(x_1 - \xi_1)^2 + (x_2 - \xi_2)^2 + (x_3 - \xi_3)^2}$, and $d\boldsymbol{\xi} = d\xi_1 d\xi_2 d\xi_3$. If we assume that the right-hand side (RHS) $f(\boldsymbol{x}, t)$ of equation (1a) is compactly supported in space-time on the domain $Q \subset \mathbb{R}^3 \times [0, +\infty)$, then formula (2) immediately implies that

$$\varphi(\boldsymbol{x}, t) \equiv 0 \quad \text{for} \quad (\boldsymbol{x}, t) \in \bigcap_{(\boldsymbol{\xi}, \tau) \in Q} \left\{ (\boldsymbol{x}, t) \big| |\boldsymbol{x} - \boldsymbol{\xi}| < c(t - \tau), \ t > \tau \right\} \quad (3)$$

The region of space-time defined by formula (3) is called *lacuna of the solution* $\varphi = \varphi(\boldsymbol{x}, t)$. This region is obviously obtained as the intersection of all characteristic cones of equation (1a) once the vertex of the cone sweeps the support of the RHS: supp $f \subseteq Q$. From the standpoint of physics, lacuna corresponds to that part of space-time, on which the waves generated by the sources $f(\boldsymbol{x}, t)$, supp $f \subseteq Q$, have already passed, and the solution has become zero again. The phenomenon of lacunae is inherently three-dimensional. The surface of the lacuna represents the trajectory of aft (trailing) fronts of the waves. The existence of aft fronts in odd-dimension spaces is known as the Huygens' principle, as opposed to the so-called wave diffusion which takes place in even-dimension spaces, see, e.g., [17]. Note that the aft fronts and the lacunae would still be present in the solution of the wave equation (1a) if the homogeneous initial conditions (1b) were replaced by some inhomogeneous initial conditions with compact support.

The notion of lacunae (or lacunas) was first introduced and studied by Petrowsky in [18] (see also an account in [19, Chapter VI]) for a variety of hyperbolic equations and systems; and general characterization of their coefficients was provided that would guarantee existence of the lacunae. However, since work [18] no constructive examples of either equations or systems have been obtained, for which lacunae would be present in the solutions, besides the actual wave equation (1a), as well as those equations that either reduce to or are derived from, the wave equation.

The group of numerical algorithms for integrating the Maxwell system of equations that we describe hereafter will be essentially based on the presence of lacunae. However, the Kirchhoff formula (2) will never be used as an actual part of the algorithm, it will only be needed at the theoretical stage, for determining the shape of the lacunae that will later be incorporated into a purely finite-difference context. Previously, the idea of using the Huygens' principle for constructing the ABCs was promoted by Ting & Miksis [20] and Givoli & Cohen [21]. Both papers, however, have suggested to use numerical quadratures to approximate the integral (2), and then couple it with the interior solver. Moreover, the approach of [20] has never been actually implemented in a practical computational setting, whereas the approach of [21] required artificial dissipation to be added to the scheme to fix the arising instabilities.

3 The Maxwell System of Equations

The propagation of electromagnetic waves in vacuum is governed by the Maxwell equations:

$$\frac{1}{c}\frac{\partial \boldsymbol{H}}{\partial t} + \nabla \times \boldsymbol{E} = \boldsymbol{0} \qquad \nabla \cdot \boldsymbol{H} = 0$$
$$\frac{1}{c}\frac{\partial \boldsymbol{E}}{\partial t} - \nabla \times \boldsymbol{H} = -\frac{4\pi}{c}\boldsymbol{j} \qquad \nabla \cdot \boldsymbol{E} = 4\pi\rho \tag{4}$$

driven by the electric charges $\rho = \rho(\boldsymbol{x}, t)$ and currents $\boldsymbol{j} = \boldsymbol{j}(\boldsymbol{x}, t)$. In system (4), $\boldsymbol{E}$ is the electric field, $\boldsymbol{H}$ is the magnetic field, c is the speed of light, and the normalization is chosen so that both the permittivity and permeability of vacuum are equal to one: $\varepsilon_0 = \mu_0 = 1$. We note that unlike the acoustics system studied in [3], all the unknown quantities in (4) are vectors.

System (4) contains a pair of unsteady equations and a pair of steady-state equations. Taking the operation curl $\equiv \nabla\times$ of one equation from the first pair, differentiating the remaining unsteady equation with respect to time, substituting into one another, and using the identity [2] $\nabla \times \nabla \times \boldsymbol{V} = -\Delta \boldsymbol{V} + \nabla(\nabla \cdot \boldsymbol{V})$ along with the corresponding steady-state equation, we arrive at the following individual equations for the fields:

$$\frac{1}{c^2}\frac{\partial^2 \boldsymbol{H}}{\partial t^2} - \Delta \boldsymbol{H} = \frac{4\pi}{c}\nabla \times \boldsymbol{j}$$
$$\frac{1}{c^2}\frac{\partial^2 \boldsymbol{E}}{\partial t^2} - \Delta \boldsymbol{E} = -4\pi \left[\frac{1}{c^2}\frac{\partial \boldsymbol{j}}{\partial t} + \nabla\rho\right] \tag{5}$$

Each of the two equations (5) is a vector wave equation. Therefore, if the currents and charges in system (4) were compactly supported in space and time, as in Section 2, then the RHSs in equations (5) would be compactly supported as well, and consequently, the solutions $\boldsymbol{E} = \boldsymbol{E}(\boldsymbol{x}, t)$ and $\boldsymbol{H} = \boldsymbol{H}(\boldsymbol{x}, t)$ *would have lacunae* of the same shape as prescribed by formula (3).

At this stage, another important difference compared to the acoustics system of equations needs to be outlined. In acoustics [3], we have required that the velocity field be conservative. It was necessary and sufficient for the individual equation for acoustic velocity to become a wave equation. [3] In its own turn, the fact that a given quantity is governed by the wave equation *is sufficient* for the solutions driven by compactly supported sources to have lacunae.

In contradistinction to that, individual equations that govern the electric and magnetic fields always reduce to the wave equation, see (5). As such, existence

---

[2] $\boldsymbol{V}$ can be any vector.
[3] The other acoustic variable, pressure, always satisfies the wave equation, [3].

of the lacunae for compactly supported sources is always guaranteed. This, however, comes "at a price." Indeed, there are two types of sources in acoustics, the volume velocity (scalar) that drives the continuity equation, and the force (vector) that drives the momentum equation. These two sources are completely independent, see [3] and also [22]. In electrodynamics, this is not the case. The currents and charges that drive the Maxwell equations (4) are always connected via the continuity equation [23]:

$$\frac{\partial \rho}{\partial t} + \nabla \cdot \boldsymbol{j} = 0 \tag{6}$$

Equation (6) may present a certain limitation when building the ABCs for the Maxwell equations (4). Indeed, our general approach [1, 2] involves construction of the special auxiliary sources that have to be compactly supported in both space and time, i.e., in the sense of Section 2. It is clear, however, that specifying a compactly supported current $\boldsymbol{j}(\boldsymbol{x}, t)$ may yield the distribution of charges $\rho(\boldsymbol{x}, t)$ that is not necessarily compactly supported in time because of equation (6). For the numerical examples of Section 8 this limitation does not manifest itself due to the cylindrically symmetric setup that we have adopted, see Sections 5 and 6. In general, however, additional attention may be required toward this issue. If, on the other hand, we knew ahead of time that the original currents, as well as charges in (4), were compactly supported, then the RHSs of (5) would be compactly supported as well, i.e., equation (6) would carry no restriction from the standpoint of existence of the lacunae.

4 Decomposition of the Original Problem

As indicated in Section 1, artificial boundary conditions are needed to truncate the problem which is originally formulated on an unbounded domain, and as such enable its solution on the computer. Suppose that the original formulation of the problem involves the entire space $\mathbb{R}^3$, but we are only interested in finding a fragment of the overall solution defined on a given domain $S(t)$. This domain has a fixed shape and finite diameter, $\operatorname{diam} S(t) = d < \infty$, for all $t \geq 0$, but is allowed to move across $\mathbb{R}^3$ according to the general law:

$$\boldsymbol{u}_0 = \boldsymbol{u}_0(t), \qquad \boldsymbol{x}_0 = \boldsymbol{x}_0(t) = \int_0^t \boldsymbol{u}_0(\tau) d\tau \tag{7}$$

where $\boldsymbol{u}_0$ and $\boldsymbol{x}_0$ are the velocity vector and coordinates of a given point inside $S(t)$, respectively. The only natural limitation is that $\max_t |\boldsymbol{u}_0(t)| = k < c$.

While not making any specific assumptions regarding the nature of the phenomena/processes that are going on inside $S(t)$, we assume that outside $S(t)$, i.e., $\forall t > 0$ and $\boldsymbol{x} \notin S(t)$, the appropriate model would be based on the

6

homogeneous Maxwell equations [cf. equations (4)]:

$$\frac{1}{c}\frac{\partial \boldsymbol{H}}{\partial t} + \nabla \times \boldsymbol{E} = \boldsymbol{0} \qquad \nabla \cdot \boldsymbol{H} = 0$$
$$\frac{1}{c}\frac{\partial \boldsymbol{E}}{\partial t} - \nabla \times \boldsymbol{H} = \boldsymbol{0} \qquad \nabla \cdot \boldsymbol{E} = 0 \tag{8}$$

We, of course, assume that the overall problem, i.e., the interior one that we do not elaborate on, combined with the exterior one, which is governed by system (8), is uniquely solvable on $\mathbb{R}^3$. In other words, our model may include some possibly complex phenomena confined to the bounded region $S(t)$ that manifest themselves by the radiation of electromagnetic waves in the far field. The objective is to actually solve the problem on the domain $S(t)$ using a numerical method, but truncate all of its exterior replacing it with the ABCs on the external boundary $\partial S(t)$. The ideal or exact ABCs would make the foregoing replacement equivalent, which means that the solution obtained this way would coincide on $S(t)$ with the corresponding fragment of the original infinite-domain solution. The latter, of course, is not actually available because the far-field propagation of electromagnetic waves governed by (8) cannot be computed directly at an acceptable cost.

Let us emphasize that from the viewpoint of an observer inside $S(t)$, the role of the ABCs at $\partial S(t)$ is only to guarantee that this boundary behave exactly as if the domain $S(t)$ were surrounded by vacuum. In particular, the boundary $\partial S(t)$ may not reflect, fully or partially, any outgoing waves. Therefore, as far as the ABCs are concerned, we indeed do not have to be very specific regarding the nature of the problem inside $S(t)$, provided, of course, that the overall interior/exterior problem does have a unique solution.

The latter assumption is obviously of key importance. However, justifying it for every particular setting is beyond the scope of the current paper. A relatively easy case would be that of linear scattering from a known (sufficiently simple) shape with known material characteristics. Otherwise, the model inside $S(t)$ may be more sophisticated, possibly nonlinear. In any event, for the purpose of constructing the ABCs, the overall solvability will hereafter be assumed, including the case when $S(t)$ is moving. We only mention that in the context of electromagnetics the capability of the method to handle moving sources of waves is probably less important than in acoustics, see [3], for the obvious reason that all feasible speeds will be much slower than the speed of light. We, however, still include this capability in the design. One reason is that there may be future applications, for which it will be important, e.g., in astrophysics. Another reason is that in electromagnetics, the structure of the field does depend on the frame of reference, in which this field is analyzed, see [23]. Again, one can, in principle, think of situations, in which employing a moving frame of reference, which, in turn, may imply moving sources, could be beneficial because of a potentially simpler structure of the associated field.

The first stage in constructing the ABCs will be decomposition of the original infinite-domain problem into two sub-problems. An auxiliary problem will be formulated that will have the exact same solution outside $S(t)$ as the original problem does, but will be linear throughout the entire space $\mathbb{R}^3$ and will be driven by the special source terms concentrated only inside $S(t)$. Next, the auxiliary problem will be solved using the lacunae-based methodology [1–3] adopted here for the Maxwell equations, and its solution obtained right outside $S(t)$ will be used to supply the boundary conditions for the interior problem solved inside $S(t)$. In practice, the two aforementioned stages will be meshed together so that both the interior problem and the auxiliary problem are time-marched concurrently. In so doing, the interior solution will be used to generate sources for the auxiliary problem, and the auxiliary solution will be used to provide the missing boundary data for the interior problem. The entire algorithm will be implemented directly on the discrete level.

Let us define a smaller subdomain $S_\varepsilon(t) \subset S(t)$ such that $\boldsymbol{x} \in S_\varepsilon(t)$ iff $\boldsymbol{x} \in S(t)$ and $\mathrm{dist}(\boldsymbol{x}, \partial S(t)) > \varepsilon$, where $\varepsilon > 0$. Let us also introduce a multiplier function $\mu = \mu(\boldsymbol{x}, t)$ that is smooth across the entire space and $\forall t > 0$ satisfies:

$$\mu(\boldsymbol{x}, t) = \begin{cases} 0, & \boldsymbol{x} \in S_\varepsilon(t) \\ 1, & \boldsymbol{x} \notin S(t) \\ \in (0, 1), & \boldsymbol{x} \in S(t) \backslash S_\varepsilon(t) \end{cases} \tag{9}$$

The curvilinear strip $S(t) \backslash S_\varepsilon(t)$ of width ϵ adjacent to the boundary $\partial S(t)$ of the domain $S(t)$ from inside will hereafter be called *the transition region.* Assume that the solution to the original problem $\boldsymbol{E}(\boldsymbol{x}, t)$, $\boldsymbol{H}(\boldsymbol{x}, t)$ is known on $\mathbb{R}^3$ for $t > 0$, and that $\boldsymbol{E}(\boldsymbol{x}, 0) = 0$ and $\boldsymbol{H}(\boldsymbol{x}, 0) = 0$ for $\boldsymbol{x} \notin S_\varepsilon(0)$, which means that nothing is going on outside the domain of interest before $t = 0$. We multiply this solution on the entire space by $\mu(\boldsymbol{x}, t)$ of (9) and obtain:

$$\begin{aligned} \boldsymbol{E}(\boldsymbol{x}, t) &\longmapsto \mu(\boldsymbol{x}, t) \boldsymbol{E}(\boldsymbol{x}, t) \equiv \hat{\boldsymbol{E}}(\boldsymbol{x}, t) \\ \boldsymbol{H}(\boldsymbol{x}, t) &\longmapsto \mu(\boldsymbol{x}, t) \boldsymbol{H}(\boldsymbol{x}, t) \equiv \hat{\boldsymbol{H}}(\boldsymbol{x}, t) \end{aligned} \tag{10}$$

We emphasize that in formulae (10) we do not, in fact, need to know $\boldsymbol{E}(\boldsymbol{x}, t)$ and $\boldsymbol{H}(\boldsymbol{x}, t)$ on $S_\varepsilon(t)$, because the multiplier μ is equal to zero there anyway. Moreover, multiplication (10) will not change any quantities on $\mathbb{R}^3 \backslash S(t)$. With that in mind, we apply the differential operators from the left-hand sides of system (8) to the modified solution $\hat{\boldsymbol{E}}(\boldsymbol{x}, t)$, $\hat{\boldsymbol{H}}(\boldsymbol{x}, t)$, see (10), and obtain:

$$\begin{aligned} -\frac{4\pi}{c} \hat{\boldsymbol{j}}_{\mathrm{m}} &:= \frac{1}{c} \frac{\partial \hat{\boldsymbol{H}}}{\partial t} + \nabla \times \hat{\boldsymbol{E}} & 4\pi \hat{\rho}_{\mathrm{m}} &:= \nabla \cdot \hat{\boldsymbol{H}} \\ -\frac{4\pi}{c} \hat{\boldsymbol{j}} &:= \frac{1}{c} \frac{\partial \hat{\boldsymbol{E}}}{\partial t} - \nabla \times \hat{\boldsymbol{H}} & 4\pi \hat{\rho} &:= \nabla \cdot \hat{\boldsymbol{E}} \end{aligned} \tag{11}$$

Relations (11) *define the auxiliary sources* $\hat{\boldsymbol{j}}_{\mathrm{m}}(\boldsymbol{x}, t)$, $\hat{\boldsymbol{j}}(\boldsymbol{x}, t)$, $\hat{\rho}_{\mathrm{m}}(\boldsymbol{x}, t)$, and

$\hat{\rho}(\boldsymbol{x}, t)$ on the space $\mathbb{R}^3$ for $t > 0$. Clearly, for $\boldsymbol{x} \in S_\varepsilon(t)$ and $t > 0$ we have:

$$\begin{aligned}
\hat{\boldsymbol{j}}_{\mathrm{m}}(\boldsymbol{x}, t) &= \boldsymbol{0} & \hat{\rho}_{\mathrm{m}}(\boldsymbol{x}, t) &= 0 \\
\hat{\boldsymbol{j}}(\boldsymbol{x}, t) &= \boldsymbol{0} & \hat{\rho}(\boldsymbol{x}, t) &= 0
\end{aligned} \tag{12}$$

because $\mu(\boldsymbol{x}, t) = 0$ for $\boldsymbol{x} \in S_\varepsilon(t)$. Equalities (12) also hold for $\boldsymbol{x} \in \mathbb{R}^3 \backslash S(t)$ and all $t > 0$, because the modified quantities $\hat{\boldsymbol{E}}(\boldsymbol{x}, t)$ and $\hat{\boldsymbol{H}}(\boldsymbol{x}, t)$ of (10) coincide with $\boldsymbol{E}(\boldsymbol{x}, t)$ and $\boldsymbol{H}(\boldsymbol{x}, t)$, respectively, on $\mathbb{R}^3 \backslash S(t)$. Therefore, the auxiliary sources (11) may only differ from zero in the transition region $S(t) \backslash S_\varepsilon(t)$. Note also that the overall smoothness of the original solution $\boldsymbol{E}(\boldsymbol{x}, t)$, $\boldsymbol{H}(\boldsymbol{x}, t)$, as well as that of the multiplier $\mu(\boldsymbol{x}, t)$, guarantee that $\hat{\boldsymbol{j}}_{\mathrm{m}}$, $\hat{\boldsymbol{j}}$, $\hat{\rho}_{\mathrm{m}}$, and $\hat{\rho}$ will be smooth compactly supported functions. In Figure 1, we schematically depict the geometry of the region on which the auxiliary sources are defined.
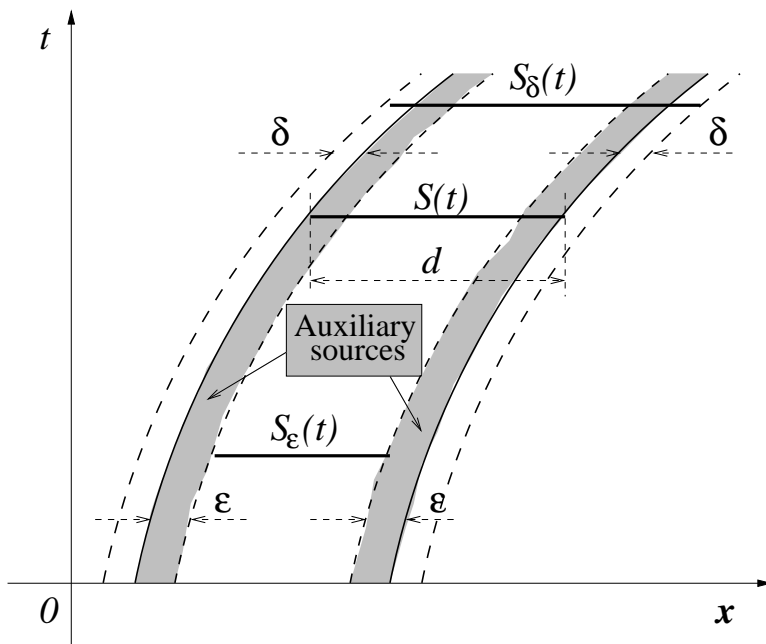

Fig. 1. Schematic geometry of the auxiliary sources region.

Similarly to the actual physical currents and charges, the electric auxiliary sources $\hat{\boldsymbol{j}}(\boldsymbol{x}, t)$ and $\hat{\rho}(\boldsymbol{x}, t)$ of (11) do satisfy the continuity equation (6), as can be verified by direct substitution. The other pair of auxiliary sources $\hat{\boldsymbol{j}}_{\mathrm{m}}$ and $\hat{\rho}_{\mathrm{m}}$ of (11) can formally be interpreted as magnetic currents and charges. They are, however, nonexistent in nature and as such shall be considered artifacts with no actual physical meaning. They are only introduced for intermediate derivation purposes, and will never be a part of any final result. The magnetic sources $\hat{\boldsymbol{j}}_{\mathrm{m}}(\boldsymbol{x}, t)$ and $\hat{\rho}_{\mathrm{m}}(\boldsymbol{x}, t)$ also satisfy the continuity equation (6).

The auxiliary problem can now be formulated: To integrate the Maxwell equations driven by the source terms (11) on the entire space subject to the homogeneous initial conditions; all equations are inhomogeneous rather than only

the second pair, as in system (4). The auxiliary problem is linear everywhere on $\mathbb{R}^3$. Under the assumption of sufficient regularity, its solution is unique. The regularity is guaranteed by the requirement that the transition from the exterior solution on $\mathbb{R}^3 \backslash S(t)$ to zero on $S_\varepsilon(t)$ be smooth, see (9) and (10), so that the auxiliary sources (11) are smooth as well. Uniqueness for the auxiliary problem implies that its solution will coincide on the entire space with the modified fields $\hat{\boldsymbol{E}}(\boldsymbol{x}, t)$ and $\hat{\boldsymbol{H}}(\boldsymbol{x}, t)$ of (10). This, in particular, means that on $\mathbb{R}^3 \backslash S(t)$ the auxiliary solution will coincide with the original exterior solution $\boldsymbol{E}(\boldsymbol{x}, t)$, $\boldsymbol{H}(\boldsymbol{x}, t)$. Note that we do not need to know the latter on $\mathbb{R}^3 \backslash S(t)$ in order to obtain the source terms $\hat{\boldsymbol{j}}_{\mathrm{m}}(\boldsymbol{x}, t)$, $\hat{\boldsymbol{j}}(\boldsymbol{x}, t)$, $\hat{\rho}_{\mathrm{m}}(\boldsymbol{x}, t)$, and $\hat{\rho}(\boldsymbol{x}, t)$ of (11) that drive the auxiliary problem. We only need to be sure that it satisfies the homogeneous Maxwell equations (8) and that transition (10) is smooth.

Altogether, we have effectively split the original problem into two: The linear auxiliary problem that needs to be solved on the entire space, and the interior problem on $S(t)$ that will be integrated with the external boundary data provided by the solution of the auxiliary problem. In their own turn, the sources that drive the auxiliary problem depend on the interior solution. The algorithm for solving the auxiliary problem will rely on the presence of lacunae in its solutions, see Sections 2 and 3. *This algorithm will allow one to keep the size of the auxiliary domain finite, computational expenses per unit time interval fixed, and accuracy non-deteriorating over long time intervals.* The lacunae-based algorithm is described in Section 6. Its implementation will, in fact, require introducing certain modifications to the formulation of the auxiliary problem. These rather minor modifications will affect the construction of the auxiliary sources so that to guarantee existence of the lacunae.

5 The Transverse-Magnetic Subsystem

From here on, we employ cylindrical coordinates (r, θ, z) in space and assume axial symmetry so that all the unknown quantities will depend only on r, z, and the time t, and $\frac{\partial}{\partial \theta}(\,\cdot\,) \equiv 0$. This facilitates the split of system (4) into two independent subsystems such that each one governs only three out of the total of six field components. The subsystem that connects E_θ, H_r, and H_z is referred to as transverse-magnetic (TM); it contains three unsteady equations

$$\frac{1}{c}\frac{\partial E_\theta}{\partial t} - \left(\frac{\partial H_r}{\partial z} - \frac{\partial H_z}{\partial r}\right) = -\frac{4\pi}{c}j_\theta$$

$$\frac{1}{c}\frac{\partial H_r}{\partial t} - \frac{\partial E_\theta}{\partial z} = 0 \tag{13a}$$

$$\frac{1}{c}\frac{\partial H_z}{\partial t} + \frac{1}{r}\frac{\partial (r E_\theta)}{\partial r} = 0$$

supplemented by the steady-state equation

$$\frac{1}{r}\frac{\partial\left(rH_r\right)}{\partial r} + \frac{\partial H_z}{\partial z} = 0 \tag{13b}$$

The latter obviously corresponds to $\nabla \cdot \boldsymbol{H} = 0$. Note that the second steady-state equation of (4), $\nabla \cdot \boldsymbol{E} = 4\pi\rho$, does not appear in the TM system because $\frac{\partial}{\partial\theta}(E_\theta) \equiv 0$. It is rather a part of the other subsystem known as transverse-electric (TE); the latter will not be considered in the current paper.

It is also known that in electrodynamics the six field components are not completely independent, they are determined by the vector and scalar potentials $\boldsymbol{A}$ and ϕ, respectively. The potentials, in their own turn, are not defined uniquely. A particular gauge [23] that we are choosing here to specify the potentials is $\boldsymbol{H} = \nabla \times \boldsymbol{A}$, $\boldsymbol{E} = -\frac{1}{c}\frac{\partial\boldsymbol{A}}{\partial t}$, $\phi \equiv 0$, which translates into

$$H_r = -\frac{\partial A_\theta}{\partial z}, \quad H_z = \frac{1}{r}\frac{\partial\left(rA_\theta\right)}{\partial r}, \quad E_\theta = -\frac{1}{c}\frac{\partial A_\theta}{\partial t} \tag{14}$$

In other words, everything is, in fact, controlled by one quantity A_θ, which is the angular component of the vector potential.

It is instrumental to compare equations (13a), (13b), and (14) with the cylindrically symmetric linearized Euler equations that appear in acoustics. If we introduce the new variables: $rA_\theta := \varphi$, $-rH_r := w$, $rH_z := u$, $rE_\theta := \frac{1}{c}p$, then system (13a) becomes

$$\frac{1}{c^2}\frac{\partial p}{\partial t} + \frac{1}{r}\frac{\partial(ru)}{\partial r}\boxed{-\frac{2}{r}u} + \frac{\partial w}{\partial z} = -\frac{4\pi}{c}rj_\theta$$
$$\frac{\partial u}{\partial t} + \frac{\partial p}{\partial r} = 0 \tag{15a}$$
$$\frac{\partial w}{\partial t} + \frac{\partial p}{\partial z} = 0$$

and equation (13b) transforms into

$$\frac{\partial u}{\partial z} - \frac{\partial w}{\partial r} = 0 \tag{15b}$$

Equality (15b) can be interpreted as the condition of zero vorticity, assuming that u and w are the radial and axial components, respectively, of the velocity vector. In that case, (15b) obviously implies conservativeness of the velocity field, which is sufficient for existence of the lacunae in the solutions of the acoustics system, see [3]. The gauge (14) is then equivalent to

$$\frac{\partial\varphi}{\partial r} = u, \quad \frac{\partial\varphi}{\partial z} = w, \quad \frac{\partial\varphi}{\partial t} = -p \tag{16}$$

11

where p should be thought of as the acoustic pressure, and φ — the velocity potential. Equalities (15b) and (16) do look, in fact, exactly the same as the corresponding relations in acoustics. Let us emphasize, however, that in spite of the substantial similarities, system (15a) is not quite identical to the actual acoustics system. The difference resides in the boxed term in the first equation of (15a), which is not present in the genuine acoustics. In fact, the two systems — two-dimensional acoustics and TM Maxwell — look completely identical only in the Cartesian coordinates. Still, the similarities that we have identified for the cylindrical coordinates will help us build the numerical algorithm for the Maxwell equations that will share certain components with the previously built procedure for the acoustics system, see [3].

Next, following the discussion of Section 4, we assume that the homogeneous version of equations (13a), (13b) [cf. formulae (8)] holds outside the domain $S(t)$. Clearly, in the cylindrically symmetric case $S(t)$ can be defined as a two-dimensional shape of variables (r, z), while the actual three-dimensional domain will be given by the corresponding body of revolution. The motion of the domain must obviously be aligned with the z-axis [cf. formulae (7)]:

$$w_0 = w_0(t), \quad z_0 = z_0(t) = \int_0^t w_0(\tau)d\tau, \quad x_0 = y_0 \equiv 0 \tag{17}$$

Inside the bounded region $S(t)$, some possibly complex processes may be going on that manifest themselves by the radiation of electromagnetic waves in the far field. We assume the overall unique solvability, introduce the multiplier $\mu = \mu(r, z, t)$ as in (9), and modify the solution on $\mathbb{R}^3$ according to (10):

$$
\begin{aligned}
E_\theta(r, z, t) &\longmapsto \mu(r, z, t) E_\theta(r, z, t) \equiv \hat{E}_\theta(r, z, t) \\
H_r(r, z, t) &\longmapsto \mu(r, z, t) H_r(r, z, t) \equiv \hat{H}_r(r, z, t) \\
H_z(r, z, t) &\longmapsto \mu(r, z, t) H_z(r, z, t) \equiv \hat{H}_z(r, z, t)
\end{aligned}
\tag{18}
$$

Then, applying the differential operators of (13a), (13b) to the modified field components of (18) we obtain the auxiliary RHSs [cf. formula (11)]:

$$
\begin{aligned}
-\frac{4\pi}{c}\hat{\jmath}_\theta &:= \frac{1}{c}\frac{\partial \hat{E}_\theta}{\partial t} - \left(\frac{\partial \hat{H}_r}{\partial z} - \frac{\partial \hat{H}_z}{\partial r}\right) \\
-\frac{4\pi}{c}\hat{\jmath}_{\mathrm{m}r} &:= \frac{1}{c}\frac{\partial \hat{H}_r}{\partial t} - \frac{\partial \hat{E}_\theta}{\partial z} \\
-\frac{4\pi}{c}\hat{\jmath}_{\mathrm{m}z} &:= \frac{1}{c}\frac{\partial \hat{H}_z}{\partial t} + \frac{1}{r}\frac{\partial \left(r\hat{E}_\theta\right)}{\partial r} \\
4\pi\hat{\rho}_{\mathrm{m}} &:= \frac{1}{r}\frac{\partial \left(r\hat{H}_r\right)}{\partial r} + \frac{\partial \hat{H}_z}{\partial z}
\end{aligned}
\tag{19}
$$

that may differ from zero only on $S(t)\backslash S_\varepsilon(t)$. The non-physical magnetic cur-

rents and charges always satisfy the continuity equation [cf. formula (6)]:

$$\frac{\partial \hat{\rho}_{\mathrm{m}}}{\partial t} + \frac{1}{r}\frac{\partial (r\hat{j}_{\mathrm{m}r})}{\partial r} + \frac{\partial \hat{j}_{\mathrm{m}z}}{\partial z} = 0 \tag{20}$$

obtained by straightforward differentiation of (19). We note that in the TM context there is no continuity equation for the electric currents and charges. The reason is that the only type of electric sources that appear in the TM mode is the current component j_θ, for which we obviously have $\frac{\partial j_\theta}{\partial \theta} \equiv 0$. The electric continuity equation is, in fact, a part of the TE subsystem.

There is also an alternative procedure for obtaining the auxiliary source terms, besides the one given by formulae (18), (19). Instead of applying the multiplier $\mu(r, z, t,)$ directly to all the field components, as done in (18), let us first reconstruct A_θ in the transition region $S(t)\backslash S_\varepsilon(t)$ using the first two equations of (14). Then, the multiplier is applied to E_θ and A_θ, and the modified magnetic filed is obtained by differentiating the modified potential:

$$E_\theta(r, z, t) \longmapsto \mu(r, z, t)E_\theta(r, z, t) \equiv \hat{E}_\theta(r, z, t)$$

$$H_r = -\frac{\partial A_\theta}{\partial z}, \quad H_z = \frac{1}{r}\frac{\partial (rA_\theta)}{\partial r} \quad \text{on} \quad S(t)\backslash S_\varepsilon(t)$$

$$A_\theta(r, z, t) \longmapsto \mu(r, z, t)A_\theta(r, z, t) \equiv \hat{A}_\theta(r, z, t) \tag{21}$$

$$H_r(r, z, t) \longmapsto -\frac{\partial \hat{A}_\theta}{\partial z} \equiv \hat{H}_r(r, z, t)$$

$$H_z(r, z, t) \longmapsto \frac{1}{r}\frac{\partial (r\hat{A}_\theta)}{\partial r} \equiv \hat{H}_z(r, z, t)$$

Replacing the straightforward modification procedure (18) by the new scheme (21) that involves reconstruction of A_θ induces important simplifications in the definition of the auxiliary RHSs (19). Namely, by adopting (21) we will guarantee that $\hat{\rho}_{\mathrm{m}} \equiv 0$, i.e., $\frac{1}{r}\frac{\partial (r\hat{H}_r)}{\partial r} + \frac{\partial \hat{H}_z}{\partial z} \equiv 0$. Besides, the continuity equation (20) will degenerate and reduce to $\frac{1}{r}\frac{\partial (r\hat{j}_{\mathrm{m}r})}{\partial r} + \frac{\partial \hat{j}_{\mathrm{m}z}}{\partial z} \equiv 0$.

Returning to the issue of comparison between electromagnetics and acoustics, we note that in three-dimensional acoustics there is no such a thing as the continuity equation for the source terms. In two dimensions, however, and in particular, in the (r, z) coordinates, an equation similar to (20) can be written that would connect the vorticity, see formula (15b), with the curl of the forcing that drives the momentum equation. In case the acoustic velocity filed is conservative, this equation degenerates similarly to the aforementioned degeneration of the continuity equation for the magnetic sources.

We should also mention that the foregoing construction of the auxiliary sources is by no means the only possible one. In fact, all we need is a smooth extension of the exterior solution inwards that would transition to zero at a given

"depth" ε, and would also maintain certain properties described in the following Section 6. There may be different ways of obtaining this extension, not necessarily based on applying the multiplier μ to the interior solution on the transition region.

6 Lacunae-Based Integration

As formulated in Section 4, the auxiliary problem consists of solving the Maxwell equations driven by the source terms (19) that are concentrated inside $S(t)$, or more precisely, on $S(t)\backslash S_\varepsilon(t)$. In other words, we need to integrate the system of equations:

$$
\begin{aligned}
\frac{1}{c}\frac{\partial E_\theta}{\partial t} - \left(\frac{\partial H_r}{\partial z} - \frac{\partial H_z}{\partial r}\right) &= -\frac{4\pi}{c}\hat{j}_\theta \\
\frac{1}{c}\frac{\partial H_r}{\partial t} - \frac{\partial E_\theta}{\partial z} &= -\frac{4\pi}{c}\hat{j}_{\mathrm{m}r} \\
\frac{1}{c}\frac{\partial H_z}{\partial t} + \frac{1}{r}\frac{\partial\left(rE_\theta\right)}{\partial r} &= -\frac{4\pi}{c}\hat{j}_{\mathrm{m}z} \\
\frac{1}{r}\frac{\partial\left(rH_r\right)}{\partial r} + \frac{\partial H_z}{\partial z} &= 4\pi\hat{\rho}_{\mathrm{m}}
\end{aligned}
\tag{22}
$$

for $t > 0$ subject to the homogeneous initial conditions. The source terms in (22) may be defined by either (18), (19) or (21), (19). The solution will need to be found on a domain slightly larger than $S(t)$ for all $t > 0$. Given $\delta > 0$, we define this new domain as $S_\delta(t) = \{(\boldsymbol{x},t)|\operatorname{dist}(\boldsymbol{x},S(t)) < \delta\}$; obviously, $S_\varepsilon(t) \subset S(t) \subset S_\delta(t)$, see Figure 1. We emphasize that the sources (19) are not independent. They can only be obtained in the context of problem decomposition, as described in Section 4. In the current section however, we will describe the solution methodology for the auxiliary problem as if those sources have simply been given. In the following Section 7, this solution methodology will be applied in the decomposition framework for actually setting the ABCs.

The definition of the source terms (18), (19) or (21), (19), along with the unique solvability, imply that the solution of system (22) will coincide with the modified fields (18) or (21), respectively. This, in particular, means that outside $S(t)$ it will coincide with the non-modified fields, as the multiplier μ is identically equal to one there, see (9).

Let us now introduce a partition of unity on the semi-infinite interval $t \geq 0$:

$$
\forall t \geq 0 : \quad \sum_{i=0}^{\infty}\Theta(t - \sigma Ti) = 1
\tag{23}
$$

where $T > 0$ and $\frac{1}{2} \leq \sigma < 1$ are two parameters, and $\Theta = \Theta(t)$ is a smooth, even, "hat"-type function with $\operatorname{supp}\Theta(t) \subseteq [-\frac{T}{2}, \frac{T}{2}]$:

$$
\Theta(t) = \begin{cases}
0, & t > \frac{T}{2} \\
1, & 0 \leq t \leq (\sigma - \frac{1}{2})T \\
1 - \Theta(\sigma T - t), & (\sigma - \frac{1}{2})T < t \leq \frac{T}{2} \\
\Theta(-t), & t < 0
\end{cases}
\tag{24}
$$

Then, we can partition the sources of (22) and obtain for $i = 0, 1, 2, \ldots$:

$$
\begin{aligned}
\hat{\hat{j}}_{\theta}^{(i)}(r,z,t) &= \hat{\hat{j}}_{\theta}(r,z,t)\Theta(t - \sigma T i), & \operatorname{supp}\hat{\hat{j}}_{\theta}^{(i)}(r,z,t) \subseteq Q_i \\
\hat{\hat{j}}_{\mathrm{m}r}^{(i)}(r,z,t) &= \hat{\hat{j}}_{\mathrm{m}r}(r,z,t)\Theta(t - \sigma T i), & \operatorname{supp}\hat{\hat{j}}_{\mathrm{m}r}^{(i)}(r,z,t) \subseteq Q_i \\
\hat{\hat{j}}_{\mathrm{m}z}^{(i)}(r,z,t) &= \hat{\hat{j}}_{\mathrm{m}z}(r,z,t)\Theta(t - \sigma T i), & \operatorname{supp}\hat{\hat{j}}_{\mathrm{m}z}^{(i)}(r,z,t) \subseteq Q_i \\
\hat{\rho}_{\mathrm{m}}^{(i)}(r,z,t) &= \hat{\rho}_{\mathrm{m}}(r,z,t)\Theta(t - \sigma T i), & \operatorname{supp}\hat{\rho}_{\mathrm{m}}^{(i)}(r,z,t) \subseteq Q_i
\end{aligned}
\tag{25}
$$

where according to (24) each domain Q_i is compact in both space and time:

$$
Q_i = \left\{ (r,z,t) \big| (r,z) \in S(t), \left(\sigma i - \frac{1}{2}\right)T \leq t \leq \left(\sigma i + \frac{1}{2}\right)T \right\}
\tag{26}
$$

Next, we would like to consider a collection of individual subsystems driven by the partitioned RHSs of (25) [cf. formulae (22)]:

$$
\begin{aligned}
\frac{1}{c}\frac{\partial E_{\theta}^{(i)}}{\partial t} - \left(\frac{\partial H_r^{(i)}}{\partial z} - \frac{\partial H_z^{(i)}}{\partial r} \right) &= -\frac{4\pi}{c}\hat{\hat{j}}_{\theta}^{(i)} \\
\frac{1}{c}\frac{\partial H_r^{(i)}}{\partial t} - \frac{\partial E_{\theta}^{(i)}}{\partial z} &= -\frac{4\pi}{c}\hat{\hat{j}}_{\mathrm{m}r}^{(i)} \\
\frac{1}{c}\frac{\partial H_z^{(i)}}{\partial t} + \frac{1}{r}\frac{\partial\left(rE_{\theta}^{(i)}\right)}{\partial r} &= -\frac{4\pi}{c}\hat{\hat{j}}_{\mathrm{m}z}^{(i)} \\
\frac{1}{r}\frac{\partial\left(rH_r^{(i)}\right)}{\partial r} + \frac{\partial H_z^{(i)}}{\partial z} &= 4\pi\hat{\rho}_{\mathrm{m}}^{(i)}
\end{aligned}
\tag{27a}
$$

For each $i = 0, 1, 2, \ldots$, the corresponding system (27a) needs to be solved for $t > (\sigma i - \frac{1}{2})T$, subject to the homogeneous initial conditions.

We need to emphasize though that the split (25), (27a) may not always be legitimate. Indeed, as can be generally shown, see [23], and as has been indicated when obtaining the source terms (19), every RHS to a Maxwell system must always satisfy the continuity equation of type (20). It is obvious that partitioning (25) may disrupt that, because multiplication by a function of time $\Theta(t - \sigma T i)$ will affect the time derivative of $\hat{\rho}_{\mathrm{m}}^{(i)}$. A natural remedy would be to use the definition of the auxiliary sources by means of formulae (21), (19) that involve the reconstruction of A_{θ} on $S(t) \backslash S_{\varepsilon}(t)$, rather than the general definition (18), (19). As has been mentioned, by using (21), (19) we guarantee

that $\hat{\rho}_{\mathrm{m}} \equiv 0$ and also independently $\nabla \cdot \boldsymbol{j}_{\mathrm{m}} \equiv 0$, so that the continuity equation (20) is satisfied identically both before the split (25) and after the split, i.e., individually for each $i = 0, 1, 2, \ldots$. As such, we will always be assuming hereafter that formulae (21), (19) have been used for defining the auxiliary sources, so that system (27a) reduces to

$$
\begin{aligned}
\frac{1}{c}\frac{\partial E_\theta^{(i)}}{\partial t} - \left(\frac{\partial H_r^{(i)}}{\partial z} - \frac{\partial H_z^{(i)}}{\partial r} \right) &= -\frac{4\pi}{c}\hat{j}_\theta^{(i)} \\
\frac{1}{c}\frac{\partial H_r^{(i)}}{\partial t} - \frac{\partial E_\theta^{(i)}}{\partial z} &= -\frac{4\pi}{c}\hat{j}_{\mathrm{m}r}^{(i)} \\
\frac{1}{c}\frac{\partial H_z^{(i)}}{\partial t} + \frac{1}{r}\frac{\partial \left(r E_\theta^{(i)} \right)}{\partial r} &= -\frac{4\pi}{c}\hat{j}_{\mathrm{m}z}^{(i)} \\
\frac{1}{r}\frac{\partial \left(r H_r^{(i)} \right)}{\partial r} + \frac{\partial H_z^{(i)}}{\partial z} &= 0
\end{aligned}
\tag{27b}
$$

where $\nabla \cdot \boldsymbol{j}_{\mathrm{m}}^{(i)} = \frac{1}{r}\frac{\partial \left(r \hat{j}_{\mathrm{m}r}^{(i)} \right)}{\partial r} + \frac{\partial \hat{j}_{\mathrm{m}z}^{(i)}}{\partial z} \equiv 0$. The RHSs of each system (27b) are compactly supported in space-time on the domain Q_i, see (26), and each of those systems is now uniquely solvable. As (23) is a partition of unity, we have:

$$
\hat{j}_\theta(r, z, t) = \sum_{i=0}^\infty \hat{j}_\theta^{(i)}(r, z, t), \qquad \hat{j}_{\mathrm{m}r}(r, z, t) = \sum_{i=0}^\infty \hat{j}_{\mathrm{m}r}^{(i)}(r, z, t),
$$

$$
\hat{j}_{\mathrm{m}z}(r, z, t) = \sum_{i=0}^\infty \hat{j}_{\mathrm{m}z}^{(i)}(r, z, t)
$$

and because of the linear superposition, the solution $E_\theta(r, z, t)$, $H_r(r, z, t)$, $H_z(r, z, t)$ of system (22) with the source terms defined by (21), (19) and subject to the homogeneous initial conditions at $t = 0$, can be expanded in terms of the solutions to systems (27b):

$$
E_\theta(r, z, t) = \sum_{i=0}^\infty E_\theta^{(i)}(r, z, t), \qquad H_r(r, z, t) = \sum_{i=0}^\infty H_r^{(i)}(r, z, t),
$$

$$
H_z(r, z, t) = \sum_{i=0}^\infty H_z^{(i)}(r, z, t)
\tag{28}
$$

The series (28) are formally infinite. However, for any $t > 0$ and $(r, z) \in S(t)$ each will, in fact, contain only a finite fixed number of nonzero terms. Indeed, due to the causality for a given $t > 0$ and all $(\sigma i - \frac{1}{2})T > t$, i.e., all $i > (\frac{t}{T} + \frac{1}{2})/\sigma$, we will have $E_\theta^{(i)}(r, z, t) = 0$, $H_r^{(i)}(r, z, t) = 0$, and $H_z^{(i)}(r, z, t) = 0$ on the entire space $\mathbb{R}^3$. Moreover, since the RHSs of system (27b) are compactly supported in space and time on the domain Q_i of (26), *solutions of this system are going to have lacunae,* as shown in Section 3. Let us now denote the moment of inception of source # i as $t_0^{(i)} = (\sigma i - \frac{1}{2})T$ and the moment of its cessation as $t_1^{(i)} = (\sigma i + \frac{1}{2})T$. Recall also that diam $S(t) = d$, which means that

diam $S_\delta(t) = d + 2\delta$, and that the maximum speed of motion of the domain $S(t)$ is $k < c$. Then, formula (3) implies that no later than

$$
\begin{aligned}
t = t_2^{(i)} = t_0^{(i)} + +\frac{d + 2\delta + (t_1^{(i)} - t_0^{(i)})(c + k)}{c - k} \\
= \left(\sigma i - \frac{1}{2}\right)T + \frac{d + 2\delta + T(c + k)}{c - k} \equiv t_0^{(i)} + T_{\text{int}}
\end{aligned}
\tag{29}
$$

all of the domain $S_\delta(t)$ will fall into the lacuna of system (27b) (see [1, 2] for a more detailed argument), and will remain inside the lacuna continuously thereafter, i.e., for all $t \geq t_2^{(i)}$. In other words, for the solution of system (27b), we will have $E_\theta^{(i)}(r, z, t) = 0$, $H_r^{(i)}(r, z, t) = 0$, and $H_z^{(i)}(r, z, t) = 0$ when $(r, z) \in S_\delta(t)$ and $t \geq t_2^{(i)}$, where $t_2^{(i)}$ is defined by formula (29). Alternatively, this means that for any $t > 0$ and all $i < (\frac{t - T_{\text{int}}}{T} + \frac{1}{2})/\sigma$, where $T_{\text{int}} = \frac{d + 2\delta + T(c+k)}{c-k}$ as in formula (29), the terms $E_\theta^{(i)}(r, z, t)$, $H_r^{(i)}(r, z, t)$ and $H_z^{(i)}(r, z, t)$ in the series (28) will be equal to zero for $(r, z) \in S_\delta(t)$. Consequently, for all $t > 0$ and $(r, z) \in S_\delta(t)$ we can replace expansions (28) with

$$
\begin{aligned}
E_\theta(r, z, t) = \sum_{i=p_1}^{p_2} E_\theta^{(i)}(r, z, t), \qquad H_r(r, z, t) = \sum_{i=p_1}^{p_2} H_r^{(i)}(r, z, t), \\
H_z(r, z, t) = \sum_{i=p_1}^{p_2} H_z^{(i)}(r, z, t)
\end{aligned}
\tag{30}
$$

where $p_1 = \left[(\frac{t - T_{\text{int}}}{T} + \frac{1}{2})/\sigma\right]$, $p_2 = \left[(\frac{t}{T} + \frac{1}{2})/\sigma\right] + 1$, and $[\cdot]$ denotes the integer part. This implies that for any $t > 0$ and $(r, z) \in S_\delta(t)$ the number of terms $p = p_2 - p_1 + 1$ in the sum (30), and as such, the number of non-zero terms in the expansion (28), may not exceed $\left[\frac{T_{\text{int}}}{\sigma T}\right] + 2$. Most important, this number p does not increase as the time t elapses, because the interval T_{int} introduced in (29) depends only on the partition size T for the sources, the diameter of the domain, the propagation speed, and the maximum speed of motion.

Next, we realize that for any given $i = 0, 1, 2, \ldots$ no wave can travel in space further away than the distance cT_{int} from the boundary of the domain $S(t_0^{(i)})$ during the time interval T_{int}. This means that we will also have $E_\theta^{(i)}(r, z, t) = 0$, $H_r^{(i)}(r, z, t) = 0$, and $H_z^{(i)}(r, z, t) = 0$ for $\text{dist}\,[(r, z), S(t_0^{(i)})] > cT_{\text{int}}$ and $t_0^{(i)} \leq t \leq t_2^{(i)}$. As such, instead of the free unobstructed space outside $S(t)$ we may consider outer boundaries with arbitrary (reflecting) properties for solving each of the problems (27b). As long as none of these boundaries is located closer than cT_{int} to $S(t_0^{(i)})$, the solution of (27b) inside $S_\delta(t)$ is not going to feel their presence for $t_0^{(i)} \leq t \leq t_2^{(i)}$.

In fact, instead of requiring that no wave may reach an outer boundary before $t = t_2^{(i)}$ we can introduce a weaker requirement that no reflected wave may come back and reach $S_\delta(t)$ before $t = t_2^{(i)}$. The latter consideration easily

translates into the following estimates for the minimal distances between the domain $S(t_0^{(i)})$ and the allowed location of any reflecting boundary, [1,2]:

$$Z_{\min} = \frac{c+k}{2}T_{\text{int}}, \quad R_{\min} = \frac{c}{2}T_{\text{int}} \tag{31}$$

Note that the minimal distances in the directions z and r are not the same, see (31), because the motion of the domain with the maximum speed k is allowed in the direction z only, see (17).

Altogether, the solution of each system (27b) driven by the sources compactly supported on the domain Q_i of (26) and subject to the homogeneous initial conditions at $t = t_0^{(i)}$, can be obtained on $S_\delta(t)$ for all $t \geq t_0^{(i)}$ as follows. First, this solution can be formally considered equal to zero for $0 \leq t \leq t_0^{(i)}$. Next, on the time interval $t_0^{(i)} < t \leq t_2^{(i)}$, see formula (29), system (27b) can be integrated on the rectangular auxiliary domain with the sides Z and R:

$$\begin{aligned}
Z &= d + 2\delta + 2Z_{\min} = d + 2\delta + (c+k)T_{\text{int}} \\
R &= d + \delta + R_{\min} = d + \delta + \frac{c}{2}T_{\text{int}}
\end{aligned} \tag{32}$$

centered around $S(t_0^{(i)})$. This is going to yield the correct solution inside $S_\delta(t)$. Finally, for all $t \geq t_2^{(i)}$ the solution on $S_\delta(t)$ will be equal to zero again because all the waves will have left the domain by $t = t_2^{(i)}$ (lacuna).

Let us now return to the representation of the solution of system (22) with the RHSs given by (21), (19) in the form of finite sums (30). Assume that the i-th component of the solution is obtained by integrating the corresponding system (27b) on the appropriate domain of size (32) by means of a consistent and stable finite-difference scheme. System (27b) only needs to be integrated from $t_0^{(i)} = (\sigma i - \frac{1}{2})T$ till $t_2^{(i)} = t_0^{(i)} + T_{\text{int}}$ because for all subsequent moments of time its solution on $S_\delta(t)$ will be equal to zero. Consequently, the following convergence estimates will hold for $t_0^{(i)} \leq t \leq t_2^{(i)}$ and $(r, z) \in S_\delta(t)$:

$$\begin{aligned}
\|E_\theta^{(i)}(r,z,t) - E_\theta^{(h,i)}(r,z,t)\| &\leq K_i h^\alpha \\
\|H_r^{(i)}(r,z,t) - H_r^{(h,i)}(r,z,t)\| &\leq K_i h^\alpha \\
\|H_z^{(i)}(r,z,t) - H_z^{(h,i)}(r,z,t)\| &\leq K_i h^\alpha
\end{aligned} \tag{33}$$

where α is the order of convergence, h denotes the generic grid size, and the functions $E_\theta^{(h,i)}(r,z,t)$, $H_r^{(h,i)}(r,z,t)$, and $H_z^{(h,i)}(r,z,t)$ denote the discrete solution of system (27b) for a given i. The stability constant K_i on the right-hand side of each inequality (33) does not depend on h, but may depend on $\hat{j}_\theta^{(i)}$, $\hat{j}_{\mathrm{m}_r}^{(i)}$, and $\hat{j}_{\mathrm{m}_z}^{(i)}$, as well as on T_{int}.

We emphasize that the quantity T_{int} does not depend on i. Moreover, it is natural to assume that the derivatives of the functions $\hat{j}_\theta^{(i)}(r,z,t)$, $\hat{j}_{\mathrm{m}_r}^{(i)}(r,z,t)$,

and $\hat{j}_{m_z}^{(i)}(r, z, t)$ are uniformly bounded with respect to i. In this case, there will be a universal, i.e., i-independent, constant $K = K(\hat{j}_\theta, \hat{j}_{m_r}, \hat{j}_{m_r}, T_{int})$ such that $\forall i = 0, 1, 2, \dots :$ $K_i \leq K$. Then, using representations (30) one can easily transform the individual convergence estimates (33) into the overall *temporally uniform* grid convergence estimate for E_θ, H_r, and H_z that would hold for $t \geq 0$ and $(r, z) \in S_\delta(t)$:

$$\|E_\theta(r, z, t) - E_\theta^{(h)}(r, z, t)\| \leq pKh^\alpha$$
$$\|H_r(r, z, t) - H_r^{(h)}(r, z, t)\| \leq pKh^\alpha \qquad (34)$$
$$\|H_z(r, z, t) - H_z^{(h)}(r, z, t)\| \leq pKh^\alpha$$

In formulae (34), $E_\theta^{(h)} = \sum\limits_{i=p_1}^{p_2} E_\theta^{(h,i)}$, $H_r^{(h)} = \sum\limits_{i=p_1}^{p_2} H_r^{(h,i)}$, and $H_z^{(h)} = \sum\limits_{i=p_1}^{p_2} H_z^{(h,i)}$, cf. formulae (30). A detailed proof of the temporally uniform grid convergence for the wave equation can be found in our previous work [1].

In practical terms, the temporally uniform grid convergence (34) means that the accuracy of the numerical solution of system (22) with the RHSs (21), (19), will not deteriorate even on arbitrarily long time intervals, if the integration is performed using lacunae, i.e., by solving the set of systems (27b) and then employing representation (30). In other words, *one should expect that there will be no long-time error buildup.* This is, in fact, a key distinction between the foregoing lacunae-based algorithm and traditional time-marching techniques that may be applied to computing the unsteady wave fields.

Indeed, the phenomenon of error accumulation during long runs is well-known in the context of computational methods for time-dependent problems. At the analysis stage, it manifests itself by the increase of the stability constants with time, which is, in fact, equivalent to non-uniformity of the grid convergence. All conventional discrete approximations that can be and are used in modern numerical methods are known to suffer from this deficiency.

As we have seen, the lacunae-based algorithm allows us to circumvent this difficulty, because even though for any individual system (27b) the stability constant K_i will still depend on the integration interval, the duration of this interval T_{int} is fixed and non-increasing for all $i = 0, 1, 2, \dots$. Moreover, the number of components, see (30), needed to obtain the solution on $S_\delta(t)$ at any given moment of time $t > 0$ is also fixed and non-increasing, which altogether translates into the temporally uniform convergence (34).

We also note that if system (22) with the RHSs given by (21), (19) were to be integrated on some large interval $[0, T_{final}]$ using a straightforward time-marching algorithm, it would have also required a large domain in space, of the size roughly $2cT_{final}$. This is typically not feasible. On the other hand, implementation of the lacunae-based algorithm allows us to perform the integration

19

on the auxiliary domain of a fixed and non-increasing size determined by formulae (32). *This is a key consideration that allows us to use the lacunae-based algorithm for setting the ABCs,* see Section 7, i.e., for obtaining computational closures when the original unbounded domain of the problem is truncated.

It is important to mention that smoothness plays a key role in the design of the lacunae-based algorithm. In particular, the function $\Theta(t)$ of (24) that helps us build the partition of unity (23) has to be chosen sufficiently smooth so that the dependence of the stability constants K_i on the properties of individual RHSs $\hat{j}_\theta^{(i)}$, $\hat{j}_{\mathrm{m}_r}^{(i)}$, and $\hat{j}_{\mathrm{m}_z}^{(i)}$, see (33), be not "worse" than that in the original scheme with non-partitioned source terms. In this paper, we leave out the detailed analysis that involves the quantitative smoothness characteristics, and instead refer the reader to our previous work [1].

Let us now address some implementation issues for the lacunae-based algorithm. In theory, system (27b) for every given $i = 0, 1, 2, \ldots$ should be integrated on its own auxiliary region of the size given by (32), centered around the domain $S(t_0^{(i)})$, where $t_0^{(i)} = (\sigma i - \frac{1}{2})T$ and the location of $S(t_0^{(i)})$ is, in turn, determined by the reference point $r = 0$, $z = z_0(t_0^{(i)})$, see formula (17). It is, however, more convenient to consider periodic boundary conditions with the period Z in the coordinate direction z. This essentially means that the motion (17) should be interpreted as motion on the circle. In so doing, all systems (27b) can basically be solved on one and the same domain of variables (r, z): $[0, R] \times [-Z/2, Z/2]$. Indeed, it does not matter where on the period the "initial" domain $S(t_0^{(i)})$ is located for every $i = 0, 1, 2, \ldots$. The boundary conditions in the r direction are discussed in Section 8.

We now recast the discrete version of formulae (30) in the form of a difference:

$$E_\theta^{(h)}(r, z, t) = \sum_{i=p_1}^{p_2} E_\theta^{(h,i)}(r, z, t) = \sum_{i=0}^{p_2} E_\theta^{(h,i)}(r, z, t) - \sum_{i=0}^{p_1-1} E_\theta^{(h,i)}(r, z, t)$$

$$H_r^{(h)}(r, z, t) = \sum_{i=p_1}^{p_2} H_r^{(h,i)}(r, z, t) = \sum_{i=0}^{p_2} H_r^{(h,i)}(r, z, t) - \sum_{i=0}^{p_1-1} H_r^{(h,i)}(r, z, t) \quad (35)$$

$$H_z^{(h)}(r, z, t) = \sum_{i=p_1}^{p_2} H_z^{(h,i)}(r, z, t) = \sum_{i=0}^{p_2} H_z^{(h,i)}(r, z, t) - \sum_{i=0}^{p_1-1} H_z^{(h,i)}(r, z, t)$$

Besides their equivalence to (30), formulae (35) can be given the following useful interpretation. The subtracted quantities $\sum_{i=0}^{p_1-1} \cdots$ in (35) are assumed zero inside the lacuna. More precisely, those are small quantities that converge to zero when the grid is refined. Therefore, their subtraction does not change the solution on $S_\delta(t)$, it rather helps halt the error buildup that would continue otherwise, i.e., if the computation of these terms were to go further on. However, outside $S_\delta(t)$ the subtracted terms correspond to the waves that

have left the domain of interest. In the presence of reflecting outer boundaries, the subtraction of $\sum\limits_{i=0}^{p_1-1}\cdots$ in (35) helps prevent those waves from coming back and re-entering the domain of interest $S_\delta(t)$ and as such, "contaminating" the solution there.

Existence of the upper limit $i = p_2$ in the summation (35) is due to the causality which is always a factor, and has nothing to do with the lacunae. Therefore, each minuend $\sum\limits_{i=0}^{p_2}\cdots$ in formulae (35) could have simply been obtained by a straightforward time-marching of system (22) on the interval $[0, t)$, with absolutely no regard to either the partition (25) or split systems (27b). Of course, neither of the full quantities $E_\theta^{(h)}(r,z,t)$, $H_r^{(h)}(r,z,t)$, or $H_z^{(h)}(r,z,t)$ can be obtained by only marching. To properly account for the presence of the subtrahends $\sum\limits_{i=0}^{p_1-1}\cdots$ in formulae (35), let us first symbolically write down the time-marching scheme that would apply to (22) and (27b):

$$E_\theta^{(h)}(r,z,t+\Delta t) = \mathcal{E}\Big(E_\theta^{(h)}(\cdot,t), H_r^{(h)}(\cdot,t), H_z^{(h)}(\cdot,t), \hat{\jmath}_\theta(\cdot,t)\Big)$$

$$H_r^{(h)}(r,z,t+\Delta t) = \mathcal{H}_r\Big(E_\theta^{(h)}(\cdot,t), H_r^{(h)}(\cdot,t), \hat{\jmath}_{\mathrm{m}r}(\cdot,t)\Big) \qquad (36)$$

$$H_z^{(h)}(r,z,t+\Delta t) = \mathcal{H}_z\Big(E_\theta^{(h)}(\cdot,t), H_z^{(h)}(\cdot,t), \hat{\jmath}_{\mathrm{m}z}(\cdot,t)\Big)$$

We assume that the boundary conditions are built into the operators $\mathcal{E}$, $\mathcal{H}_r$ and $\mathcal{H}_z$. Note, scheme (36) is chosen two-level explicit for simplicity only, this is by no means a limitation, and the analysis for multi-level schemes can be found in [1]. Consider now a particular moment of time t that corresponds to the change in the lower summation limit in formulae (35) from $i = p_1$ to $i = p_1 + 1$, i.e., such t that

$$\underbrace{\left[\Big(\frac{t+\Delta t - T_{\mathrm{int}}}{T} + \frac{1}{2}\Big)/\sigma\right]}_{p_1+1} = \underbrace{\left[\Big(\frac{t - T_{\mathrm{int}}}{T} + \frac{1}{2}\Big)/\sigma\right]}_{p_1} + 1. \qquad (37)$$

Combining formulae (35) and (36), we will then have for this particular t:

$$\begin{aligned}
E_\theta^{(h)}(\cdot,t+\Delta t) &= \mathcal{E}\Big(E_\theta^{(h)}(\cdot,t), H_r^{(h)}(\cdot,t), H_z^{(h)}(\cdot,t), \hat{\jmath}_\theta(\cdot,t)\Big) \\
&\quad - E_\theta^{(h,p_1)}(\cdot,t+\Delta t) \\
H_r^{(h)}(\cdot,t+\Delta t) &= \mathcal{H}_r\Big(E_\theta^{(h)}(\cdot,t), H_r^{(h)}(\cdot,t), \hat{\jmath}_{\mathrm{m}r}(\cdot,t)\Big) - H_r^{(h,p_1)}(\cdot,t+\Delta t) \quad (38) \\
H_z^{(h)}(\cdot,t+\Delta t) &= \mathcal{H}_z\Big(E_\theta^{(h)}(\cdot,t), H_z^{(h)}(\cdot,t), \hat{\jmath}_{\mathrm{m}z}(\cdot,t)\Big) - H_z^{(h,p_1)}(\cdot,t+\Delta t)
\end{aligned}$$

In other words, when the current moment of time t satisfies the "switch" condition (37), the terms $E_\theta^{(h,p_1)}(r,z,t+\Delta t)$, $H_r^{(h,p_1)}(r,z,t+\Delta t)$, and $H_z^{(h,p_1)}(r,z,t+$

Δt) need to be explicitly subtracted from the respective overall expressions, see (38), *on top of the standard time-marching step* as per (36). This basically amounts to the required change of the upper summation limit in both subtrahends of formulae (35) from $p_1 - 1$ to p_1. We will also assume hereafter that similarly to the original differential equations (22), the scheme (36) satisfies the linear superposition principle. Then, the next time step after the one defined by formulae (38), i.e., the step $t + \Delta t \longmapsto t + 2\Delta t$, shall only be done by marching (36). Indeed, the subtracted quantities $E_\theta^{(h,p_1)}(r, z, t + \Delta t)$, $H_r^{(h,p_1)}(r, z, t + \Delta t)$, and $H_z^{(h,p_1)}(r, z, t + \Delta t)$ will carry over to all the steps that follow (38) due to the linearity. The genuine "unperturbed" marching can thus continue till the next switching moment t, i.e., till condition (37) is satisfied by $p_1 + 2$ and $p_1 + 1$. At this moment, the quantities $E_\theta^{(h,p_1+1)}(r, z, t + \Delta t)$, $H_r^{(h,p_1+1)}(r, z, t + \Delta t)$, and $H_z^{(h,p_1+1)}(r, z, t + \Delta t)$ will need to be subtracted, and then the procedure will cyclically repeat itself.

We therefore conclude that the lacunae-based algorithm can be implemented as a conventional time-marching procedure supplemented by repeated subtraction of the retarded terms, see (38). The subtraction moments can be determined ahead of time and are separated from one another by equal time increments. The subtracted terms are legitimately called retarded because for a given moment of time t that satisfies (37), they are generated by the RHSs that are active in the past, on the time interval $[t_0^{(p_1)}, t_0^{(p_1)} + T] = [(\sigma p_1 - \frac{1}{2})T, (\sigma p_1 + \frac{1}{2})T] = [t - T_{\text{int}}, t - T_{\text{int}} + T]$. Of course, the actual subtracted quantities $E_\theta^{(h,p_1+1)}(r, z, t + \Delta t)$, $H_r^{(h,p_1+1)}(r, z, t + \Delta t)$, and $H_z^{(h,p_1+1)}(r, z, t + \Delta t)$ shall be re-computed for every p_1 independently of the primary time-marching procedure. This is done by means of the same scheme (36) applied to the corresponding system (27b) on the interval $[t - T_{\text{int}}, t]$.

7   Setting the ABCs

Assume that there is a space-time grid $\mathbb{N} \times \mathbb{T}$, on which a discrete approximation to the auxiliary problem is built. The spatial grid $\mathbb{N}$ consists of the nodes $\boldsymbol{n}$, whereas the temporal grid $\mathbb{T}$ is composed of the time levels $l = 0, 1, 2, \ldots$. Note that in the case of a staggered scheme (see the example in Section 8) each "formal" node $(\boldsymbol{n}, l)$ may, in fact, correspond to a collection of several space-time locations, each associated with a different variable, that are shifted with respect to one another in a particular way. The grid $\mathbb{N}$ is actually introduced on the auxiliary domain $[0, R] \times [-Z/2, Z/2]$ of size (32). We emphasize that the grid $\mathbb{N}$ does not have to offer any special geometric features to accommodate the shape of the domain $S(t)$. It is most convenient to simply use a uniform Cartesian grid. We also note that the original problem solved inside $S(t)$ does not have to be approximated on the same grid. In the most gen-

eral situation, we will have different grids for the interior problem and for the exterior/auxiliary problem. Then, in the transition region $S(t)\backslash S_\varepsilon(t)$ we may need to employ a chimera-type grid strategy, i.e., interpolate in-between the overlapping grids. For the analysis in the current paper, however, we will simply assume that the quantities from the interior solution are already available on the grid sub-domain $\{\mathbb{N} \times \mathbb{T}\} \cap \{S(t)\backslash S_\varepsilon(t)\}$.

Let us denote by $\mathbb{N}^l$, $l = 0, 1, 2, \ldots$, the corresponding time levels of the grid $\mathbb{N} \times \mathbb{T}$, and by $\mathbb{S}^l_{\boldsymbol{n}}$ the stencil of the scheme associated with the node $(\boldsymbol{n}, l) \in \mathbb{N} \times \mathbb{T}$. For simplicity, we will assume that the auxiliary problem (22), (21), (19) is time-marched by an explicit scheme, and that the node $(\boldsymbol{n}, l) \in \mathbb{S}^l_{\boldsymbol{n}}$ is the actual upper-level node on the $m + 1$-level stencil, i.e., $\mathbb{S}^l_{\boldsymbol{n}} \cap \{\mathbb{N} \times \mathbb{T}\} \subset \{\mathbb{N}^l \cup \mathbb{N}^{l-1} \cup \ldots \cup \mathbb{N}^{l-m}\}$ and $\mathbb{S}^l_{\boldsymbol{n}} \cap \mathbb{N}^l = (\boldsymbol{n}, l)$. In Section 6, we have assumed $m = 1$, see formula (36). Denote by $\mathbb{N}^l_+$ the sub-grid of $\mathbb{N}^l$ that belongs to the interior domain, i.e., $\mathbb{N}^l_+ = \mathbb{N}^l \cap S(t^l)$, where t^l is the l-th time level in actual units ("seconds"); in the simplest case $t^l = l\Delta t$. Then, introduce the sum of the interior sub-grids for all time levels: $\mathbb{N}_+ = \mathbb{N}^0_+ \cup \mathbb{N}^1_+ \cup \mathbb{N}^2_+ \cup \ldots \subset \mathbb{N} \times \mathbb{T}$. Finally, consider a somewhat larger sub-grid of $\mathbb{N} \times \mathbb{T}$: $\tilde{\mathbb{N}}_+ = \underset{(\boldsymbol{n},l)\in\mathbb{N}_+}{\cup} \mathbb{S}^l_{\boldsymbol{n}}$, which is simply a composition of all the stencils $\mathbb{S}^l_{\boldsymbol{n}}$ obtained when the upper-level node $(\boldsymbol{n}, l)$ sweeps the grid $\mathbb{N}_+$; obviously, $\mathbb{N}_+ \subset \tilde{\mathbb{N}}_+$. The part of the grid $\tilde{\mathbb{N}}_+$ that does not belong to $\mathbb{N}_+$ is called *the grid boundary* and is denoted $\gamma = \tilde{\mathbb{N}}_+\backslash\mathbb{N}_+$. We will require that the domain $S_\delta(t^l)$ be chosen so that on every time level t^l, $l = 0, 1, 2, \ldots$, all of the grid $\tilde{\mathbb{N}}^l_+$ belong to this domain: $\tilde{\mathbb{N}}^l_+ \subset S_\delta(t^l)$; equivalently, we may require that $\gamma^l \subset S_\delta(t^l)$. We note that the grid boundary γ is a narrow fringe of grid nodes that follows the geometry of $\partial S(t)$. Therefore, the parameter δ may be chosen small, on the order of a few grid sizes depending on the specific structure of the stencil $\mathbb{S}^l_{\boldsymbol{n}}$. We also note that our construction of the grid boundary γ is a simplified interpretation of the rigorous general definition that is used for obtaining the discrete Calderon's potentials and boundary projection operators [24]; the latter are used in [16] as a universal apparatus for setting the ABCs.

We will now describe one time step of the combined time-marching algorithm that involves setting the lacunae-based ABCs. In so doing, we will assume that all time steps are identical and as such, will provide an inductive description of the algorithm. In other words, all the operations performed on a given time step will be assumed to have been performed on all the previous steps as well.

Suppose that we have obtained the solution for up to a given time level l. This means that the solution is known not only on the interior domain, but also on the grid boundary — at the levels $\gamma^l, \ldots, \gamma^{l-m}$ that are immediately needed for advancing the next time step, as well as at all the preceding levels. In particular, one may think about starting the computation from the known (homogeneous) initial conditions. First, we make one interior time step and

23

obtain the discrete solution everywhere inside $S(t)$ including the transition region, i.e., the grid area $\mathbb{N}^{l+1} \cap \{S(t^{l+1}) \backslash S_\varepsilon(t^{l+1})\}$. Then, we perform the modification (21) in the discrete framework, which involves, among other things, reconstruction of A_θ on the grid in the transition region $S(t^{l+1}) \backslash S_\varepsilon(t^{l+1})$. The most straightforward approach to do that is contour integration along the grid lines; it has proven quite robust in our simulations, see Section 8, taking in to account, of course, that the potential A_θ only needs to be reconstructed on a narrow near-boundary strip. Having gotten the modified quantities (21) on the grid sub-domain $\mathbb{N}^{l+1} \cap \{S(t^{l+1}) \backslash S_\varepsilon(t^{l+1})\}$, we apply the discrete version of (19) [introduced in Section 8] and obtain one more time level of the discrete auxiliary RHSs. If the scheme written on the stencil $\mathbb{S}_n^l$ approximates system (22) with the design accuracy at some node $(\boldsymbol{n} - \boldsymbol{n}_0, l - l_0) \in \mathbb{S}_n^l$ (clearly, $l_0 \leq m$), then the discrete RHSs should obviously be referred to this same node $(\boldsymbol{n} - \boldsymbol{n}_0, l - l_0)$ and as such, advancing the interior solution till $(l + 1)$ would mean building the auxiliary RHSs till $(l + 1 - l_0)$. Next, we make one time step for the auxiliary problem with these newly updated RHSs, and obtain its solution on $\mathbb{N}^{l+1}$. Since we have chosen $\delta > 0$ so that $\tilde{\mathbb{N}}_+^{l+1} \subset S_\delta(t^{l+1})$, we determine that the solution to the auxiliary problem will, in particular, be available on γ^{l+1}. This concludes one full time step, because once we know the solution on all time levels up to $(l+1)$ everywhere including the grid boundary, we can advance the next interior time step, etc.

We should emphasize that the auxiliary problem is solved by the lacunae-based methodology of Section 6. The latter includes cyclic subtractions (38) of the retarded terms defined by the partition (25) on top of the straightforward time-marching. It is important to realize that once a particular component has been subtracted, there will never be a need to analyze/incorporate it again in the course of computation. In other words, the subtracted terms are completely disregarded from the moment of subtraction further on. Therefore, the corresponding partition elements (25) of the auxiliary RHSs can be disregarded as well. Consequently, even when integrating over arbitrarily long time intervals, we only need to keep a finite amount of the past information, namely, the auxiliary RHSs (19) defined on the interval of duration T_{int}, see (29), that immediately precedes the current moment of time. This makes *the extent of temporal nonlocality* of the proposed ABCs *fixed and limited.*

Summarizing on the implementation strategy, we time-march the combined problem by performing the alternating interior/auxiliary steps. To advance an interior step, we need the data on the grid boundary γ, i.e., at those nodes of the scheme stencil that do not belong to the interior domain. Providing these missing data basically means setting the discrete ABCs. This is done in practice by computing the solution to the auxiliary problem on the finite domain $[0, R] \times [-Z/2, Z/2]$ of size (32), which, in particular, means obtaining it at the grid boundary γ as well. The latter solution is, in turn, driven by the source terms that are generated based on the interior solution.

In the end of the section, we outline the important design features of the new unsteady ABCs. The boundary conditions are built directly in the discrete framework and can be constructed for any given scheme. The computational expenses per unit time still remain fixed and non-growing. The outer boundary becomes completely transparent for all the outgoing waves, and the accuracy of the boundary treatment is fully determined by that of the scheme employed. The fixed and non-growing expenses per time step are accounted for by using the lacunae-based integration. Besides, the lacunae-based approach guarantees that the ABCs, while being nonlocal, still have only limited and non-growing extent of temporal nonlocality. In addition to that, the accuracy of the boundary treatment per se will not deteriorate as the time elapses. Finally, the ABCs have the capability of handling moving domains, including those engaged in an accelerated motion. In the following Section 8, we corroborate the foregoing design properties of the proposed ABCs by actual numerical examples.

8 Numerical Demonstrations

For the purpose of constructing a discretization, it will be necessary to write the TM Maxwell system on the axis of symmetry $r = 0$. First of all, we note that all the unknown quantities must be continuous and bounded everywhere. For the vector components E_θ and H_r this consideration, along with the axial symmetry, imply that both E_θ and H_r must be equal to zero at $r = 0$. The same will obviously be true for A_θ. For the vector component H_z, which is parallel to the axis of symmetry, the same arguments lead to the conclusion that $\frac{\partial H_z}{\partial r}\big|_{r=0} = 0$. Next, using Taylor's expansion for $r \ll 1$, we have: $E_\theta(r, \cdot) = E_\theta'(0, \cdot) r + o(r)$ and consequently, $\frac{1}{r}\frac{\partial(r E_\theta)}{\partial r} = \frac{1}{r}\frac{\partial(r^2 E_\theta'(0, \cdot))}{\partial r} + o(1)$, which means that $\frac{1}{r}\frac{\partial(r E_\theta)}{\partial r}\big|_{r=0} = 2\frac{\partial E_\theta}{\partial r}\big|_{r=0}$. Therefore, for $r = 0$ system (22) transforms into:

$$
\begin{aligned}
E_\theta(0, z, t) &= 0 \\
H_r(0, z, t) &= 0 \\
\frac{1}{c}\frac{\partial H_z}{\partial t} + 2\frac{\partial E_\theta}{\partial r} &= 0 \\
2\frac{\partial H_r}{\partial r} + \frac{\partial H_z}{\partial z} &= 0
\end{aligned}
\tag{39}
$$

which, in particular, implies that the RHSs (21), (19) are equal to zero on the axis. The gauge definition (14) for $r = 0$ becomes:

$$
H_z = 2\frac{\partial A_\theta}{\partial r}
\tag{40}
$$

25

The domain $S(t)$ is chosen as a ball of fixed diameter d centered on the z axis, with its center moving according to (17). Obviously, as the motion (17) is aligned with the direction $r = 0$, it does not break the axial symmetry. The value for the diameter that we take is $d = 1.8$; the functions $w_0(t)$, and $z_0(t)$ of (17) will be specified later. The value for the speed of light is chosen $c = 1$.

The auxiliary domain is a rectangle $[0, R] \times [-Z/2, Z/2]$ of variables (r, z), with the actual sizes $R = \pi$ and $Z = 2\pi$. We make sure that the other parameters σ, T, and δ, see (29), are chosen so that these sizes be greater or equal to the corresponding minimal values prescribed by (32). The boundary conditions in the z direction are periodic:

$$
\begin{aligned}
E_\theta(r, z \pm Z, t) &= E_\theta(r, z, t) \\
H_r(r, z \pm Z, t) &= H_r(r, z, t) \\
H_z(r, z \pm Z, t) &= H_z(r, z, t)
\end{aligned} \tag{41a}
$$

The boundary conditions in the radial direction obviously cannot be periodic because of the geometry/symmetry considerations. At $r = 0$, there is no need for special boundary treatment at all; instead, we have the first two equations of (39) along with $\left.\frac{\partial H_z}{\partial r}\right|_{r=0} = 0$. At $r = R$, the boundary conditions are needed for the homogeneous counterpart of system (22), and we set:

$$
\left.\frac{\partial(rE_\theta)}{\partial r}\right|_{r=R} = 0, \quad \left.\frac{\partial(rH_r)}{\partial r}\right|_{r=R} = 0, \quad H_z(R, z, t) = 0 \tag{41b}
$$

We note that the particular reflecting properties of boundary conditions (41a) and (41b) are basically immaterial from the standpoint of reconstructing the infinite-domain solution on $S(t)$, as long as the geometric restrictions discussed in Section 6 are honored. We only need to make sure that the auxiliary problem is uniquely solvable, which boundary conditions (41a), (41b) do provide for. We leave out a detailed justification of the latter statement, only mention that the homogeneous Robin boundary condition (41b) for E_θ follows from the homogeneous Dirichlet boundary condition (41b) for H_z combined with the homogeneous counterpart of the third equation of (22); and the homogeneous Robin boundary condition (41b) for H_r follows from the homogeneous Dirichlet boundary condition (41b) for H_z combined with the homogeneous counterpart of the fourth (steady-state) equation of (22).

To validate the proposed numerical method, a test solution is needed. Construction of the test solution for electromagnetics will be somewhat more elaborate than that for acoustics, see [3]. In acoustics, we have been able to build the test solution by first obtaining the velocity potential, which is a genuine scalar function. In the context of electrodynamics, the quantity A_θ that determines all the fields according to (14) is rather a component of a vector. In the TM mode, this component may not depend on the polar angle θ.

We start with constructing two auxiliary dipole solutions ψ_x and ψ_y of the three-dimensional scalar wave equation:

$$\frac{1}{c^2}\frac{\partial^2\{\psi_x,\psi_y\}}{\partial t^2} - \Delta\{\psi_x,\psi_y\} = \chi(t)\{\delta_x,\delta_y\}(x,y,z-z_0(t)) \qquad (42)$$

where in each case the RHS is a point dipole oriented either along x or along y, which travels according to the law (17) and has a time-dependent amplitude $\chi(t)$. Solutions of equation (42) can be obtained by computing convolutions with the fundamental solution of the wave operator, which is a single layer of unit magnitude on the expanding sphere of radius ct, see [3] and [25, Chapter 7] for detail. To write down ψ_x and ψ_y in a convenient form, let us introduce a new function $\tilde{r} = \tilde{r}(t) \stackrel{\text{def}}{=} \sqrt{r^2 + (z - z_0(t))^2}$ and denote $\nu = \tilde{r}(\tau) + c\tau$, where τ is a parameter. Then,

$$\begin{aligned}
\psi_{\{x,y\}}(r,z,t) = &\ \frac{1}{4\pi}\frac{c\{x,y\}\chi'(\tau)}{[c\tilde{r}(\tau) - (z - z_0(\tau))w_0(\tau)]^2}\bigg|_{\nu=ct} \\
&+ \frac{c\{x,y\}\chi(\tau)}{4\pi}\Bigg[\frac{c}{\tilde{r}(\tau)[c\tilde{r}(\tau) - (z - z_0(\tau))w_0(\tau)]^2} \\
&- \frac{-\frac{c(z-z_0(\tau))w_0(\tau)}{\tilde{r}(\tau)} + w_0^2(\tau) - (z - z_0(\tau))w_0'(\tau)}{[c\tilde{r}(\tau) - (z - z_0(\tau))w_0(\tau)]^3}\Bigg]\Bigg|_{\nu=ct}
\end{aligned} \qquad (43)$$

The right-hand side of equality (43) has to be evaluated for $\nu = ct$, i.e., for

$$\sqrt{r^2 + (z - z_0(\tau))^2} + c\tau = ct \qquad (44)$$

Solution τ of the algebraic equation (44) gives the actual retarded moment of time, at which the trajectory of the traveling point source intersects the lower portion of the characteristic cone with the vertex (r, z, t). For the case of a uniform motion, equation (44) is quadratic with respect to τ and can be solved in the closed form. Its root $\tau < t$, once substituted in (43), yields solution of the wave equation that can also be obtained via the Lorentz transform. This approach was adopted in [1, 2] for the case of monopole sources. In general however, one should not expect to be able to solve the nonlinear equation (44) explicitly. For the simulations in the current paper, equation (44) is solved numerically using the Newton method.

Next, we know that the vector potential $\boldsymbol{A}$ satisfies the (vector) wave equation, see [23]. Therefore, its Cartesian components should individually satisfy the standard scalar wave equations. Let us now define $A_x = \psi_y$ and $A_y = \psi_x$, see (42). Then, expressing the angular component of the potential as $A_\theta =$

27

$A_x \sin \theta + A_y \cos \theta$ we obtain:

$$A_\theta(r,z,t) = \frac{cr}{4\pi} \frac{1}{[c\tilde{r}(\tau) - (z - z_0(\tau))w_0(\tau)]^2} \left[\chi'(\tau) + \chi(\tau) \left(\frac{c}{\tilde{r}(\tau)} \right. \right.$$
$$\left. \left. - \frac{-\frac{c(z-z_0(\tau))w_0(\tau)}{\tilde{r}(\tau)} + w_0^2(\tau) - B(z - z_0(\tau))w_0'(\tau)}{c\tilde{r}(\tau) - (z - z_0(\tau))w_0(\tau)} \right) \right] \Bigg|_{\nu=ct} \tag{45}$$

Expression (45) obviously gives an appropriate, i.e., axially symmetric, A_θ. To actually evaluate it for a given (r, z, t), the corresponding retarded moment τ needs to be determined. Assuming that $k_1 \leq w_0(t) \leq k_2$, where k_1 and k_2 are known, we solve equation (44) by Newton's method with the initial guess τ_0 given by the solution of the quadratic equation:[4] $r^2 + (z - \frac{1}{2}(k_1 + k_2)\tau_0)^2 = c(t - \tau_0)^2$ that satisfies $\tau_0 < t$. For the numerical demonstrations in this paper, we specify the same law of motion (17) as we used in acoustics, see [3]:

$$z_0(t) = \left[\frac{t}{10} \right] + \frac{1}{2} \left(1 + \frac{15}{8} s - \frac{5}{4} s^3 + \frac{3}{8} s^5 \right), \quad s = 2 \left(\left\{ \frac{t}{10} \right\} - \frac{1}{2} \right), \tag{46}$$

where $[\,\cdot\,]$ denotes the integer part, as before, and $\{\,\cdot\,\}$ denotes the fractional part. The motion (46) consists of repeated acceleration/deceleration cycles of duration 10, so that during each cycle the source travels a total distance of 1 along the z axis. Both the velocity $w_0(t) = z_0'(t)$ and the acceleration $w_0'(t) = z_0''(t)$ determined by (46) are continuous functions of time, and $0 = k_1 \leq w_0(t) \leq k_2 = 0.1875$, which means that the condition $\max_t |w_0(t)| < c$ is met because $c = 1$.

Solution (45) for the potential A_θ is obviously singular, and cannot be used directly to derive the quantities needed for testing the numerical procedure. To remove the singularity, we introduce a smooth function $G = G(\tilde{r})$, $\tilde{r} = \tilde{r}(t)$, such that $G(\tilde{r}) \equiv 1$ for $\tilde{r} \geq \frac{\kappa d}{2}$, where $\kappa < 1$, and also such that $\frac{d^k G(0)}{d\tilde{r}^k} = 0$ for $k = 0, \ldots, 4$. Then, the new function $A_\theta(r, z, t) \cdot G(\tilde{r})$ is continuous and bounded everywhere. By differentiating it, we define the components of the reference solution to the cylindrical TM system [cf. formulae (14)]:

$$E_\theta(r, z, t) = -\frac{1}{c} \frac{\partial}{\partial t} \left(A_\theta(r, z, t) \cdot G(\tilde{r}) \right)$$
$$H_r(r, z, t) = -\frac{\partial}{\partial z} \left(A_\theta(r, z, t) \cdot G(\tilde{r}) \right) \tag{47}$$
$$H_z(r, z, t) = \frac{1}{r} \frac{\partial}{\partial r} \left(r \cdot A_\theta(r, z, t) \cdot G(\tilde{r}) \right)$$

On the axis $r = 0$, we use the first two relations of (39) and formula (40). Note that A_θ of (45) is a retarded potential, and therefore differentiating it as in (47)

---

[4] Obtained from (44) for the case of a uniform motion with the speed $(k_1 + k_2)/2$.

will involve implicit differentiation of τ via equation (44). In contradistinction to that, the definition of $G(\tilde{r})$ does not involve any retardation.

The variables E_θ, H_r, and H_z of (47) satisfy the homogeneous Maxwell system for $\tilde{r} > \frac{\kappa d}{2}$, i.e., outside a smaller ball concentric with $S(t)$. The value of κ that we took for our simulations was $\kappa = 0.8$. Inside this smaller ball, i.e., for $\tilde{r} \leq \frac{\kappa d}{2}$, E_θ, H_r, and H_z of (47) satisfy equations (13a), (13b) with the current j_θ obtained by directly substituting the field components (47) into the first equation of the system. Note, when removing the singularity of the solution we have required that sufficiently many derivatives of G be equal to zero at $\tilde{r} = 0$; consequently, the resulting j_θ will have no singularities either. Altogether, we have therefore obtained *a reference electromagnetic solution, which is regular everywhere, and which can be said to be generated by the electric currents concentrated inside the moving domain $S(t)$*, more precisely, on a smaller concentric ball of diameter κd. Outside of this smaller ball, our reference solution is basically a system of unsteady electromagnetic waves radiated by and propagating away from a moving source. We are going to reconstruct this solution numerically on the domain $S(t)$, and set the discrete lacunae-based ABCs on its outer boundary $\partial S(t)$ according to the methodology of Sections 7 and 6. The latter will include formulating the interconnected interior and auxiliary problems, building the near-boundary auxiliary RHSs, and integrating the auxiliary problem using the lacunae-based algorithm.

The Maxwell system (13a) is approximated numerically on the Cartesian grid of variables (r, z):

$$
\begin{aligned}
r_i &= i\Delta r, \quad \Delta r = R/N_r, \quad i = 0, 1, \dots, N_r \\
z_j &= j\Delta z, \quad \Delta z = Z/2N_z, \quad j = 0, \pm 1, \dots, \pm N_z
\end{aligned}
\tag{48}
$$

using a second-order staggered finite-difference scheme:

$$
\frac{1}{c}\frac{E_{\theta_{i,j}}^{l+1} - E_{\theta_{i,j}}^{l}}{\Delta t} + \frac{H_{z_{i+\frac{1}{2},j}}^{l+\frac{1}{2}} - H_{z_{i-\frac{1}{2},j}}^{l+\frac{1}{2}}}{\Delta r} -
$$
$$
\frac{H_{r_{i,j+\frac{1}{2}}}^{l+\frac{1}{2}} - H_{r_{i,j-\frac{1}{2}}}^{l+\frac{1}{2}}}{\Delta z} = -\frac{4\pi}{c} j_{\theta_{i,j}}^{l+\frac{1}{2}}
$$
$$
\frac{1}{c}\frac{H_{r_{i,j+\frac{1}{2}}}^{l+\frac{1}{2}} - H_{r_{i,j+\frac{1}{2}}}^{l-\frac{1}{2}}}{\Delta t} - \frac{E_{\theta_{i,j+1}}^{l} - E_{\theta_{i,j}}^{l}}{\Delta z} = 0
$$
$$
\frac{1}{c}\frac{H_{z_{i+\frac{1}{2},j}}^{l+\frac{1}{2}} - H_{z_{i+\frac{1}{2},j}}^{l-\frac{1}{2}}}{\Delta t} + \frac{1}{r_{i+\frac{1}{2}}}\frac{r_{i+1}E_{\theta_{i+1,j}}^{l} - r_i E_{\theta_{i,j}}^{l}}{\Delta r} = 0
$$

$$\tag{49a}$$

Note that we do not include the discretized equation (13b) into the integration scheme (49a). From the structure of system (13a) it is easy to conclude that if

equation (13b) holds for $t = 0$, which is always the case for the homogeneous initial conditions, it will also hold for all subsequent $t > 0$. This property is, in fact, inherited by the staggered discretization (49a), as can be verified directly, assuming that the discrete derivatives for (13b) are done in a natural way consistent with (49a). Note also that the auxiliary system (27b) is discretized using the same scheme (49a). The only difference is that the second and third equations may be inhomogeneous, the corresponding discrete RHSs $\hat{j}_{\mathrm{m}r}^{(i)}$ and $\hat{j}_{\mathrm{m}z}^{(i)}$ are referred to the grid locations $(i, j + \frac{1}{2}, l)$ and $(i + \frac{1}{2}, j, l)$, respectively. The discrete version of the last equation of (27b) does not have to be a part of the integration scheme either. Indeed, as indicated in Section 7 all the auxiliary RHSs are obtained directly on the discrete level, i.e., by applying the corresponding difference operators to the modified fields on the grid, similarly to (19). In so doing, if the modification (21) is used, then the appropriate discrete version of the degenerate continuity equation $\frac{1}{r}\frac{\partial(r\hat{j}_{\mathrm{m}r})}{\partial r} + \frac{\partial\hat{j}_{\mathrm{m}z}}{\partial z} = 0$ will guarantee that once the discretized last equation of (27b) holds for the initial data, it will hold for all subsequent moments of time as well.

Scheme (49a) is, in fact, a version of the well-known Yee scheme that was originally introduced for solving the Cartesian Maxwell equations, see [26]. Discretization (49a) is valid for $i > 0$, i.e., away from the axis of symmetry. On the axis, we discretize equations (39), which yields:

$$E_{\theta_{0,j}}^l = 0$$
$$H_{r_{0,j+\frac{1}{2}}}^{l+\frac{1}{2}} = 0$$
$$\frac{1}{c}\frac{H_{z_{\frac{1}{2},j}}^{l+\frac{1}{2}} - H_{z_{\frac{1}{2},j}}^{l-\frac{1}{2}}}{\Delta t} + \frac{2}{\Delta r}E_{\theta_{1,j}}^l = 0 \tag{49b}$$

Periodic boundary conditions (41a) are recast on the grid as follows:

$$E_{\theta_{i,N_z}}^l = E_{\theta_{i,-N_z}}^l, \quad H_{r_{i,N_z+\frac{1}{2}}}^{l+\frac{1}{2}} = H_{r_{i,-N_z+\frac{1}{2}}}^{l+\frac{1}{2}}, \quad H_{z_{i+\frac{1}{2},N_z}}^{l+\frac{1}{2}} = H_{z_{i+\frac{1}{2},-N_z}}^{l+\frac{1}{2}} \tag{50a}$$

whereas boundary conditions (41b) are discretized as:

$$\frac{r_{N_r}E_{\theta_{N_r,j}}^l - r_{N_r-1}E_{\theta_{N_r-1,j}}^l}{\Delta r} = 0, \quad \frac{r_{N_r}H_{r_{N_r,j+\frac{1}{2}}}^{l+\frac{1}{2}} - r_{N_r-1}H_{r_{N_r-1,j+\frac{1}{2}}}^{l+\frac{1}{2}}}{\Delta r} = 0$$
$$H_{z_{N_r-\frac{1}{2},j}}^{l+\frac{1}{2}} = 0 \tag{50b}$$

A staggered second-order scheme similar to (49a), (49b) has been used for conducting the numerical experiments with lacunae-based ABCs in acoustics, see [3]. There are, however, important differences, not only in the structure of the system, see (15a), but also in how the variables are assigned to the integer

and semi-integer grid nodes, and how the continuous and discrete boundary conditions in the radial direction are set.

Four our simulations of the Maxwell equations, we have used a sequence of three successively more fine square cell grids, $\Delta r = \Delta z$, of dimensions $N_r \times 2N_z = 64 \times 128$, 128×256, and 256×512. The Courant stability constraint was applied when selecting the time step for the explicit scheme (49a), (49b). The grid boundary γ was built in accordance with the definition given in Section 7, taking into account that scheme (49a), (49b) is staggered. The latter implies that we effectively have three independent stencils that are shifted with respect to one another for updating one electric field component and two magnetic field components. Of course, the grid boundary is constructed concurrently with the actual time-marching. The parameter δ that is needed to accommodate the width of the grid boundary γ was taken $\delta = \frac{3}{2}\Delta r$. The functions $\Theta(t)$, $\mu(\boldsymbol{x}, t)$, and $G(\tilde{r})$ introduced in order to guarantee smoothness at all the stages of the derivation, are constructed as piece-wise polynomials with four continuous derivatives everywhere. In so doing, the multiplier $\mu(\boldsymbol{x}, t)$, see (9), is also built as only a function of $\tilde{r}$. The amplitude $\chi(t)$, which is a part of the definition of the potential A_θ, see (45), was chosen in the form of a harmonic oscillation with the frequency three times that of the motion cycles (46). The width ε of the transition region $S(t) \backslash S_\varepsilon(t)$, see Figure 1, varied to demonstrate different aspects of the algorithm performance, see below. The parameter σ, which is a part of the definition of the partition of unity (23), (24) was chosen $\sigma = \frac{3}{4}$. The actual temporal thickness T of each partition element was calculated "backwards" from (29) and (32), considering that the domain size, the maximum motion speed, see (46), and the period Z are known. When marching the auxiliary problem, retarded components of the solution are subtracted according to (38). Each subtracted component is recomputed as solution to the corresponding problem (27b). For a given i, this problem is inhomogeneous on the interval $[t_0^{(i)}, t_1^{(i)}] \equiv [(\sigma i - \frac{1}{2})T, (\sigma i + \frac{1}{2})T]$, and then it remains homogeneous on the interval $[t_1^{(i)}, t_2^{(i)}] \equiv [(\sigma i + \frac{1}{2})T, (\sigma i - \frac{1}{2})T + T_{\text{int}}]$. Therefore, we first explicitly time-march this system on its interval of inhomogeneity. Then, we do the FFT of the solution in the z direction and expansion with respect to the corresponding eigenfunctions (evaluated numerically) in the r direction, which allows us to advance the homogeneous solution further till $t_2^{(i)}$ by simply raising the resulting amplifications factors to the corresponding powers. We note that in so doing scheme (49a) effectively gets split into three discrete wave equations for the respective unknown quantities. The reason is that because of the cylindrical geometry different transforms along r are needed for different variables. This is basically the only instance at which reduction to a set of independent wave equations is employed; and it is only necessitated by a particular choice of the coordinate system, which allows us to take advantage of the three-dimensional effects in a two-dimensional computational setting.
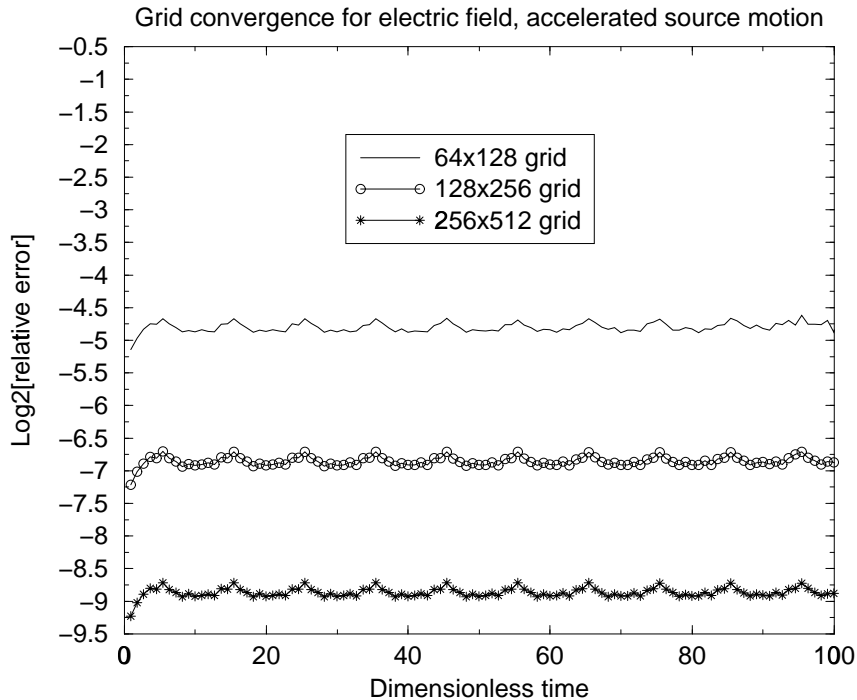
Fig. 2. Grid convergence study with lacunae-based ABCs, $\varepsilon = 10\Delta r$.

In Figure 2 we present the computational error for E_θ as it depends on time on all three grids that we have employed. The total integration time was $100\frac{d}{c}$, i.e., one hundred times the interval required for the waves to cross the domain. The error was evaluated in the maximum norm on the domain $S(t)$. We see that the algorithm provides for no long-term error buildup, and also that it displays the design second-order grid convergence. Error profiles for both magnetic filed components H_r and H_z look practically the same and we are not showing them here.

Similarly to our analysis in acoustics [3], we will now discuss how the performance of the lacunae-based ABCs is affected by the key parameter involved — the width of the transition region $S(t)\backslash S_\varepsilon(t)$ defined Section 4. This width ε obviously reflects on how well the smooth multiplier function $\mu(\boldsymbol{x}, t)$ is resolved on the grid, and as such, how smooth the auxiliary RHSs (19) will effectively be. The latter, in turn, affect the quality of the discrete lacunae, i.e., how sharp the aft fronts of the waves really are in the discrete framework. This is important because every time a retarded component is subtracted, see (38), we assume that what is being subtracted inside the lacuna, i.e., on the domain $S_\delta(t)$, is zero, or more precisely, a small quantity that converges to zero with the refinement of the grid; the convergence, however, hinges on the smoothness of the source terms. Besides having a potential effect on the error behavior, the width of the transition region also determines how many
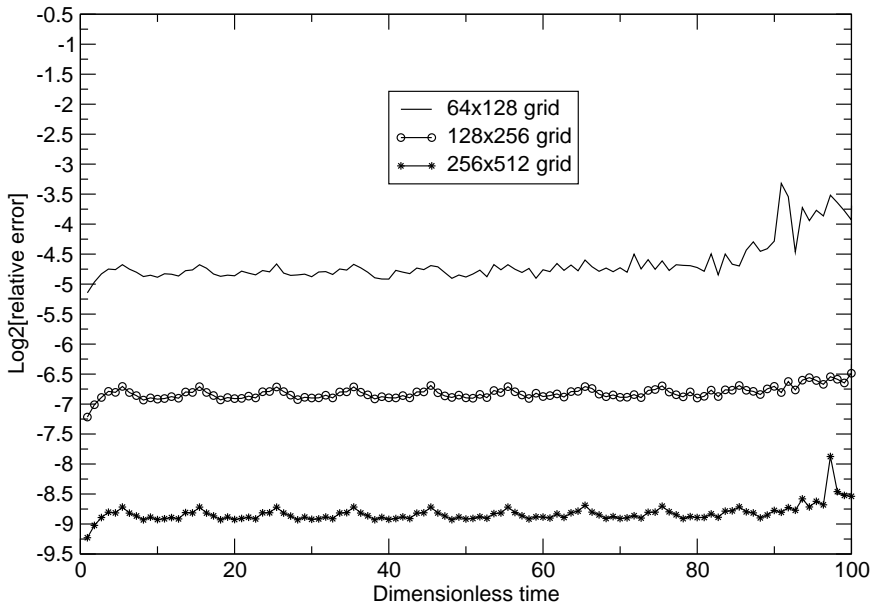
32

Fig. 3. Grid convergence study with lacunae-based ABCs, $\varepsilon = 8\Delta r$.

grid nodes are needed to support the auxiliary RHSs. We remind that those RHSs basically control the extent of temporal nonlocality of the lacunae-based ABCs. The algorithm requires keeping them on the interval of length T_{int} that immediately precedes the current moment of time, and as such, the more narrow the transition region is, the less additional storage is needed.

The error curves on Figure 2 were obtained for the transition region $S(t)\backslash S_{\varepsilon}(t)$ being relatively wide, on the order of ten grid cell sizes. In so doing, the actual geometric width of $S(t)\backslash S_{\varepsilon}(t)$ decreases with the refinement of the grid. We are, however, interested to find out what happens when the number of cells in the transition region also decreases. In Figures 3, 4, 5, and 6 we are showing the E_{θ} error profiles for the width of the transition region being $\varepsilon = 8$, 6, 4, and 2 grid cell sizes, respectively.

We observe that with the decrease of ε the error deteriorates, which is natural to expect. We also notice, though, that the deterioration is more visible on the coarser grids, whereas on the finest grid that we have employed, 256×512, it is much slower. Qualitatively, this is the same type of behavior as we have seen in acoustics, see [3]. There is also an important difference. In acoustics, when ε decreases, all the error profiles start to grow more or less monotonically with time, see [3]. The smaller the ε the faster this growth is, although on the finest grid it is not as fast as on the coarser grids. In contradistinction to that, in the current electromagnetic context the error profile on the finest grid always remains flat on some initial time interval, after which it starts to deteriorate. The extent of this initial interval decreases with the decrease
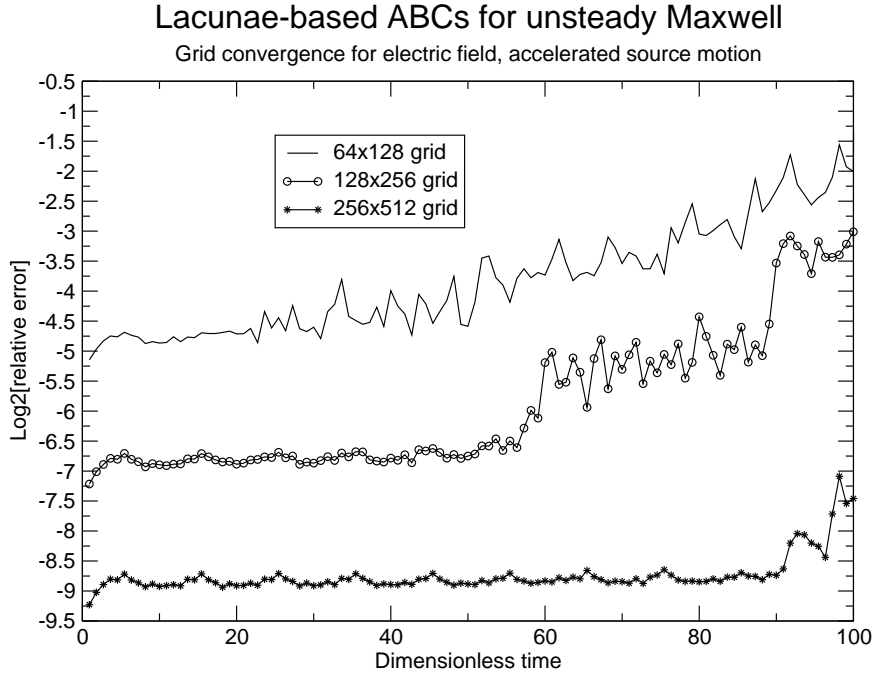
33

Lacunae-based ABCs for unsteady Maxwell
Grid convergence for electric field, accelerated source motion

Fig. 4. Grid convergence study with lacunae-based ABCs, $\varepsilon = 6\Delta r$.

Lacunae-based ABCs for unsteady Maxwell
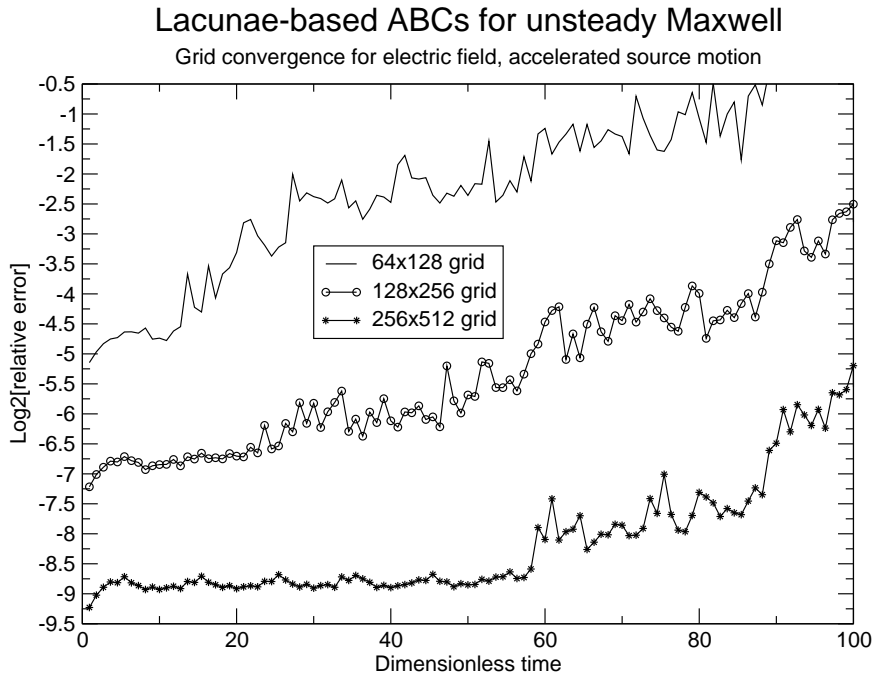### Grid convergence for electric field, accelerated source motion

Fig. 5. Grid convergence study with lacunae-based ABCs, $\varepsilon = 4\Delta r$.

of ε, but even for the narrowest transition region that we have considered, $\varepsilon = 2\Delta r$, it is still quite substantial, about 30 units, i.e., 30 times the time needed for the waves to cross the domain, see Figure 6. The presence of this initial flat portion of the error profile is beneficial as it essentially means that the lacunae-based ABCs can be used for a certain period of time *with no*
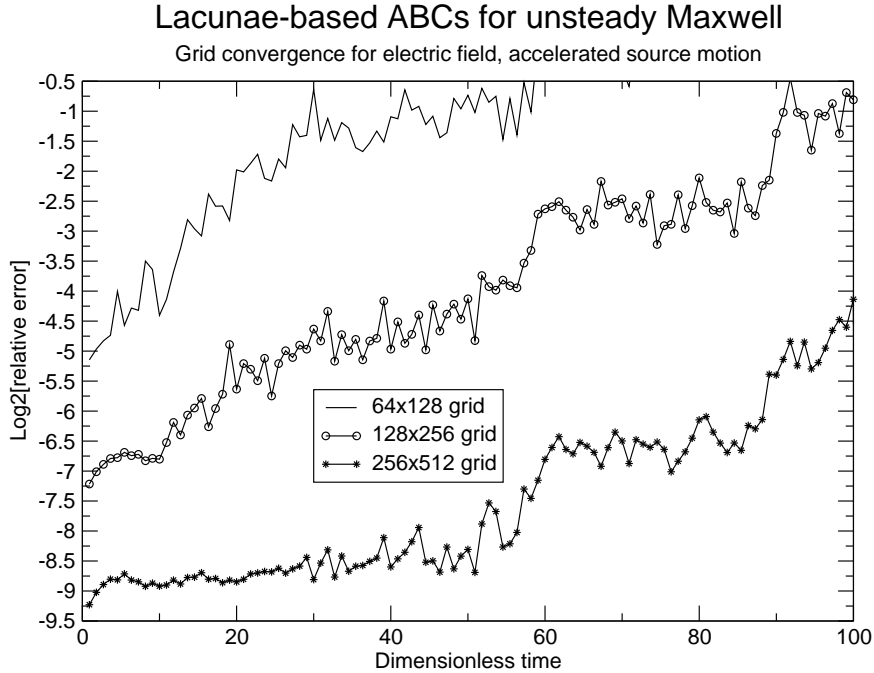
34

Fig. 6. Grid convergence study with lacunae-based ABCs, $\varepsilon = 2\Delta r$.

deterioration of performance even when the auxiliary RHSs involved are not really smooth. We note that having only two grid sizes across $S(t)\backslash S_\varepsilon(t)$ does imply that there is no smoothing in the transition region at all. We are rather having a sharp truncation, and effectively substituting an equivalent of the Heaviside function on the grid for the multiplier $\mu(\boldsymbol{x}, t)$.

As of yet, we cannot offer a rigorous theoretical explanation of why the algorithm appears more sensitive to the quality of the discrete lacunae on coarser grids than on the fine grid. To some extent this is counterintuitive because a typical instability would rather manifest itself by a rapid deterioration of the solution when the grid is refined. We can only "speculate" that the observed behavior has to do with the actual magnitude of those discrete "tails" behind the aft fronts of the waves that are due to the "imperfections" in the auxiliary sources, and that apparently are still smaller on fine grids. Altogether, this phenomenon is certainly advantageous for computations with lacunae-based ABCs, because fine grids are needed for high overall accuracy anyway, and at the same time they will allow to maintain high accuracy of the boundary treatment for longer periods of time.

9 Discussion

We have constructed and tested the algorithm for setting highly-accurate global artificial boundary conditions for the computation of time-dependent

35

electromagnetic waves. This work extends our previous approach that applies to the scalar wave equation [2], and is also similar to the ABCs that we have recently developed for unsteady acoustics [3]. The algorithm is based on the presence of lacunae (aft fronts of the waves) in the three-dimensional wave-type solutions. The ABCs are obtained directly for the discrete formulation of the problem and can complement any consistent and stable finite-difference scheme. In so doing, neither a rational approximation of non-reflecting kernels, nor discretization of the continuous boundary conditions is required, see the review [5]. The extent of temporal nonlocality of the new ABCs appears fixed and limited, and this is not a result of any approximation but rather a direct consequence of the fundamental properties of the solution. The proposed ABCs can handle artificial boundaries of irregular shape on regular grids with no fitting/adaptation needed. Besides, they possess a unique capability of being able to handle boundaries of moving computational domains, including the case of accelerated motion.

The key idea of using lacunae for computations is straightforward: *One should not continue the computation inside the lacuna once the solution has become zero there due to "natural causes."* Otherwise the error may unwarrantably build up on one hand, and on the other hand, the extent of the required temporal pre-history of the solution may grow un-justifiably high.

Of course, there are many technical issues that need to be addressed before this idea can actually be implemented in practice. Those relate primarily to what to do with the waves outside, rather than inside, the domain of interest. In the framework of the previous analysis, we simply allow them to propagate a certain distance away till they get reflected, and then set up the auxiliary domain so that the reflected waves do not reach the domain of interest before it completely falls inside the lacuna. This, however, is by no means the only possible option. In fact, any treatment of the outgoing waves that would prevent the reflections from re-entering the domain of interest before it falls into the lacuna will be appropriate. At the same time, introducing an alternative to the approach described above may be beneficial from the standpoint of the overall computational cost. For example, a treatment of the sponge layer type that slows down the outgoing waves, see, e.g., [27, 28], may allow to reduce the size of the auxiliary domain. Alternatively, the lacunae-based approach can be combined with a PML-based treatment for the waves outside the domain of interest, see, e.g., the survey papers [29, 30].

The scope of numerical demonstrations presented in the current paper is limited to the cylindrically symmetric case. The reason for that is two-fold. On one hand, by doing so we can take advantage of the fundamentally important three-dimensional effects in an essentially two-dimensional computational setting. We have, in fact, followed this strategy in our previous work on acoustics [3] and on the scalar wave equation [2]. On the other hand, cylindrically

symmetric TM mode helps us guarantee that the partitioned auxiliary sources will satisfy the correct continuity equation, see the beginning of Section 6. For that purpose we also need to use a particular method of obtaining the auxiliary sources that involves reconstruction of the potential component A_θ. Reconstruction of A_θ in the context of electromagnetics is similar to reconstruction of the velocity potential that we have used in acoustics, see [3]. In electromagnetics, however, it is needed to ensure the solvability the auxiliary sub-problems with the partitioned RHSs (27b), whereas in acoustics existence of the potential implies existence of the lacunae in the solutions of the auxiliary problem. We should note that in the full-fledged electromagnetics context that involves all six field components (as opposed to the TM subsystem that governs only three components) there will be both the magnetic continuity equation and the electric continuity equation for the RHSs that will need to be enforced once the sources are partitioned in time. At this moment of time, the question of how it may be achieved for the electric part remains open. To some extent, this presents an obstacle for constructing the lacunae-based ABCs for the Maxwell equations in the most general case. Of course, this obstacle can be easily overcome by simply reducing the system to a collection of six individual wave equations for the field components, and treating each equation independently from the others according to the methodology of [2]. This always remains a "fail-safe" option; it may, however, be more expensive than obtaining the ABCs in the framework of one first-order system. As such, implementation for the full three-dimensional Maxwell system will be in the focus of the future study.

For the current cylindrically symmetric case, numerical experiments conducted in the paper fully corroborate the theoretical design properties of the method. Besides, when a key parameter of the algorithm, the width of the transition region, changes so that to reduce the overall memory requirements, the performance of the ABCs deteriorates in an expected way. However, on fine grids this deterioration is considerably slower than that on coarse grids. Therefore, for those practical problems, for which typical integration times are sufficiently long but not excessively long, this deterioration my go almost unnoticed.

References

[1] V. S. Ryaben'kii, S. V. Tsynkov, V. I. Turchaninov, Long-time numerical computation of wave-type solutions driven by moving sources, Appl. Numer. Math. 38 (2001) 187–222.

[2] V. S. Ryaben'kii, S. V. Tsynkov, V. I. Turchaninov, Global discrete artificial boundary conditions for time-dependent wave propagation, J. Comput. Phys. 174 (2) (2001) 712–758.

[3] S. V. Tsynkov, Artificial boundary conditions for the numerical simulation of unsteady acoustic waves, J. Comput. Phys. Submitted for publication.

[4] D. Givoli, Non-reflecting boundary conditions, J. Comput. Phys. 94 (1991) 1–29.

[5] T. Hagstrom, Radiation boundary conditions for the numerical simulation of waves, in: A. Iserlis (Ed.), Acta Numerica, Vol. 8, Cambridge University Press, Cambridge, 1999, pp. 47–106.

[6] S. V. Tsynkov, Numerical solution of problems on unbounded domains. A review, Appl. Numer. Math. 27 (1998) 465–532.

[7] M. J. Grote, J. B. Keller, On nonreflecting boundary conditions, J. Comput. Phys. 122 (1995) 231–243.

[8] M. J. Grote, J. B. Keller, Exact nonreflecting boundary conditions for the time-dependent wave equation, SIAM J. Appl. Math. 55 (1995) 280–297.

[9] M. J. Grote, J. B. Keller, Nonreflecting boundary conditions for time-dependent scattering, J. Comput. Phys. 127 (1996) 52–65.

[10] M. J. Grote, J. B. Keller, Nonreflecting boundary conditions for Maxwell's equations, J. Comput. Phys. 139 (1998) 327–342.

[11] I. L. Sofronov, Artificial boundary conditions of absolute transparency for two- and three-dimensional external time-dependent scattering problems, European J. Appl. Math. 9 (1998) 561–588.

[12] I. L. Sofronov, Non-reflecting inflow and outflow in a wind tunnel for transonic time-accurate simulations, J. Math. Anal. Appl. 221 (1998) 92–115.

[13] B. Alpert, L. Greengard, T. Hagstrom, Rapid evaluation of nonreflecting boundary kernels for time-domain wave propagation, SIAM J. Numer. Anal. 37 (2000) 1138–1164.

[14] B. Alpert, L. Greengard, T. Hagstrom, Nonreflecting boundary conditions for the time-dependent wave equation, J. Comput. Phys. 180 (1) (2002) 270–296.

[15] E. Michielssen, A. Ergin, B. Shanker, D. Weile, The multilevel plane wave time domain algorithm and its applications to the rapid solution of electromagnetic scattering problems: A review, in: Mathematical and numerical aspects of wave propagation (Santiago de Compostela, 2000), SIAM, Philadelphia, PA, 2000, pp. 24–33.

[16] V. S. Ryaben'kii, Nonreflecting time-dependent boundary conditions on artificial boundaries of varying location and shape, Appl. Numer. Math. 33 (2000) 481–492.

[17] V. S. Vladimirov, Equations of Mathematical Physics, Dekker, New-York, 1971.

[18] I. Petrowsky, On the diffusion of waves and the lacunas for hyperbolic equations, Matematicheskii Sbornik (Recueil Mathématique) 17 (59) (3) (1945) 289–370.

[19] R. Courant, D. Hilbert, Methods of Mathematical Physics. Volume II, Wiley, New York, 1962.

[20] L. Ting, M. J. Miksis, Exact boundary conditions for scattering problems, J. Acoust. Soc. Am. 80 (1986) 1825–1827.

[21] D. Givoli, D. Cohen, Nonreflecting boundary conditions based on Kirchhoff-type formulae, J. Comput. Phys. 117 (1995) 102–113.

[22] J. Lončarić, S. V. Tsynkov, Optimization of acoustic source strength in the problems of active noise control, SIAM J. Applied Math. To appear. Also: Tech. Report No. 2002–11, NASA/CR–2002–211636, ICASE, Hampton, VA, May 2002.

[23] L. D. Landau, E. M. Lifshitz, The Classical Theory of Fields, Pergamon Press, Oxford, 1962.

[24] V. S. Ryaben'kii, Method of Difference Potentials and Its Applications, Springer-Verlag, Berlin, 2002.

[25] P. M. Morse, H. Feshbach, Methods of Theoretical Physics. Parts I and II, McGraw-Hill, Boston, 1953.

[26] K. S. Yee, Numerical solution of initial boundary value problem involving Maxwell's equations in isotropic media, IEEE Trans. Antennas Propagat. 14 (1966) 302–307.

[27] M. Israeli, S. Orszag, Approximation of radiation boundary conditions, J. Comput. Phys 41 (1981) 115–135.

[28] S. Karni, Far-field filtering operators for suppression of reflections from artificial boundaries, SIAM J. Numer. Anal. 33 (1996) 1014–1047.

[29] S. Abarbanel, D. Gottlieb, On the construction and analysis of absorbing layers in CEM, Appl. Numer. Math. 27 (1998) 331–340.

[30] E. Turkel, A. Yefet, Absorbing PML boundary layers for wave-like equations, Appl. Numer. Math. 27 (1998) 533–557.